1. INTRODUCTION

1.1 General

Masonry infill walls are frequently used as interior partitions and exterior walls in buildings. The performance of such structures during an earthquake has attracted major attention. Even though frame-infill interaction has sometimes led to undesired structural performance, recent studies have shown that a properly designed frame with infill wall can be superior to a bare frame in terms of stiffness, strength, and energy dissipation.

The out-of-plane vibration of infill panels can have a beneficial effect on the global response by reducing the participating mass in the fundamental modes of vibration, and hence all global response parameters; however the possible expulsion ***(sudden failure)*** is of some concern for large panels at high storey ***(Calvi G. Michele, Bolognini Davide and Penna Andrea; University of Pavia, Italy)***. Especially on a very slender infill wall, the most unfavorable condition may occur when the seismic input direction is orthogonal to the plane of the wall itself, because the large deflections, consequent to small lateral stiffness, amplify second order effects ***(instability)***, implying an instability risk.

It may be noted that masonry panels are not expected to have any effect on the strength of RC frame, when they are subjected to normal ***(Out-of-plane)*** loading. So, only stability of the masonry is to be evaluated in normal direction. Out-of-plane behavior of infill walls is a local action and is to be studied separately. The in-plane failure may not right away lead to collapse since the load carrying capacity of wall is not completely lost by diagonal cracking. However, out-of-plane failure leads to explosive collapse and may be the cause of many casualties.

Nepal National Building Code ***(NBC 201:1994)*** states that ***"To prevent masonry walls between framing columns from falling out, these shall be provided with horizontal reinforced concrete (RC) bands through the wall at about one-third and two-third of their height above the floor in each storey" (clause: 8.1.1).*** This code recommends the monolithic construction of RC band and structural columns and the trend of such construction is wide spreading day by day especially in those municipalities where the National Building Code is being imposed. These RC bands obviously increase the stability of infill wall by reducing wall span vertical direction. ***Fig-A1***

1.2 Problems and issues

The predominant and largely beneficial effect of masonry infill on the lateral response of structures has for long been recognized by researchers, yet the role of infill as earthquake resisting elements is often ignored by design engineers.

In Spite in general infill masonry wall has positive significance on the response of frame structure construction and hence such type of construction is widely recommended. But in such type of constructions, the infill wall behaves as almost as free standing wall because the bond between the infill wall and the structural elements like beam, column etc. is very weak. While analyzing and designing building with RC frames, the behavior of such infill wall is generally ignored and however if taken into account the emphasis is given for the case of in plane loading. Every designer puts his efforts toward strengthening the structural frames and no or less effort toward infill wall. But in reality the infill wall is frequently subjected to extreme out-of-plane loading especially during seismic shaking. Since the stiffness as well as rigidity of the frame element in orthogonal direction is not much more in comparison with infill wall and also the infill wall is much slender in general, there is every possibility of falling out of the masonry wall as shown in ***Fig-A2.*** The walls are brittle and tend to collapse during earthquakes, causing injuries and even loss of life even if the properly designed structural RC frames may be in proper condition after extensive shaking. ***Fig-A3***

A common type of construction in urban areas is RC framed structures with infill masonry wall ***(not reinforced)***. The construction trend is mostly prioritizing infill frame ***(first frame construction and later walls)*** as shown in ***Fig-A4*** and not confined masonry ***(walls first and beam column later or simultaneously)***. But the behavior of both could be quite different as in confined masonry wall is under compression and there exists quite good bond between wall and beam/column where as in infill frame it is doubtful.

As per ***FEMA 356*** permissible height-to-thickness (h_{inf}/t_{inf}) ratios for infill wall is given in ***table-1***. Out-of-plane analysis shall not be required for infill with h_{inf}/t_{inf} ratios less than the values listed herein.

Table 1: Maximum h_{inf}/t_{inf} Ratios

Low seismic zone	Moderate seismic zone	High seismic zone
14	13	8

Commonly the height of infill wall is 2.7 m i.e. c/c distance of beams is 3 m and the depth beam is 0.3 m. In Nepal most of the brick infill walls are half brick thick; i.e. thickness of infill wall is 0.115 m. So the ratio of height to thickness of infill wall is approximately 23. Even if the infill wall is one brick thick, the height to thickness of infill wall would be approximately 12. Since Nepal lies in high seismic zone, out-of-plane analysis is most essential.

While analyzing RC frames proper attention should be given toward the contribution of infill wall to resist seismic load as well as due care should be given toward the stability of the wall itself for both in plane as well as out-of-plane loading condition. Stability during out-of-plane loading is more critical in comparison to during in plane loading because during in plane loading, the infill wall tends to resist load in combination with RC frame i.e. role of RC frame is significant and also the stiffness of wall for in plane loading is very high but during out-of-plane loading the infill wall, in general, resist load individually i.e. role of RC frame is insignificant and also the stiffness of wall for out-of-plane loading is very low. So to have a proper technique of

analyzing the infill wall for the case of out-of-plane loading is the matter of importance.

As specified above National Building Code ***(NBC 201:1994)*** emphasized to provide RC structural bands to prevent out-of-plane failure. National Building Code is being imposed in municipalities by the government and hence the construction with RC structural bands is being increasing. The RC bands tie the wall with RC frame elements and create a support for walls loaded along weak direction. But its beneficial contribution toward out-of-plane stability is not known quantitatively. So a difficulty has to be faced to convince the concerned people about its importance.

Also due to the monolithic construction of RC bands with column, there is likelihood of changing structural response (moment, shear, axial force etc) RC frames during extreme shaking. Short column effect may also be induced due to the presence of such RC bands. Hence study on change structural performance of RC frames if any in quantitative way is also being necessary. Therefore above issues and problems can be stated as follows:

i. There is no trend to analyze the out of plane response of infill wall while designing building and less attention is given toward its stability.
ii. Contribution of RC bands in preventing out-of-plane failure of infill wall is not known in quantitative figure.
iii. No explicit understanding about the effect of RC band on structural performance of structural elements under ground shaking.

This thesis work tends to deal with these problems and issues.

1.3 Objective

1.3.1 Overall objective

The overall objective of this research work is to study the significance of RC bands suggested by ***NBC 201:1994*** in preventing the out-of-plane failure of infill wall numerically.

1.3.2 Specific objectives

The specific objectives of this proposed research work are as follows:

i. Formulation of suitable finite element model to analyze the infill wall.
ii. Study on the contribution of RC bands in preventing the out-of-plane failure by carrying out the comparison on stresses on bricks, mortar etc. and relative displacement of bricks, mortar etc.
iii. Study on crack pattern of the infill walls in comparative way for both types of models (with and without RC bands).
iv. Study on change in behavior of structural elements due to presence of RC bands, i.e. change in magnitudes of different stresses on the bounding frames, to see whether the presence of RC bands affect the bounding frames or not.

1.4 Scope and limitation of the study

To achieve the objective of study, first of all a proper numerical model has to be prepared, appropriate material properties has to be assigned, analysis of the model has to be carried out and results have to be interpreted carefully. The scope of this thesis work will be as per follows:

i. Geometric configuration of the building has been adopted as per the limitation specified by Nepal National Building Code ***(NBC 201:1994).***
ii. Study has been concentrated on only one panel.
iii. Micro modeling has been carried out for the concerned panel only and macro modeling have been carried out for other infill walls as well as frames; i.e. all other infill walls have been modeled as equivalent strut and all other frames have been modeled as single solid elements. The aim of such modeling is only to take approximately into account the stiffness of other walls and RC frames.
iv. Except the concentrated infill panel and its bounding frames, the output results of all other elements have been discarded.
v. The concentrated infill wall has no opening.

vi. Material properties have been taken from standard literature.

vii. Direct integration non-linear time history analysis has been carried out taking a famous earthquake El Centro.

viii. Time step of 0.005 sec. has been taken for direct integration time history analysis. If full acceleration history of El Centro earthquake was taken, the number of steps of integration would be very high which takes huge time duration in analyzing the model that is practically difficult to achieve using normal computer in normal working environment. So major acceleration history of early period has been taken into account and minor acceleration history of later period has been discarded.

ix. Analysis has been carried out using software SAP 2000.

x. Study has been carried out for two cases (with and without RC bands) to get comparative results.

xi. The mortar has been modeled as link elements. The non linearity in the link element has been considered assigning link element as plastic (Kinematics) spring. Though the mortar will not behave in this way, the link is selected to approximate the non linearity which is the best option available in SAP 2000.

xii. Comparative study has been carried out for the peak response only i.e. at time period at which response is largest; it is because the comparison of results at each step of analysis is practically infeasible.

xiii. Bond strength between mortar and brick and mortar and concrete has been assumed same.

1.5 Methodology

In order to arrive at specified objectives following methodologies have been followed:

a) Literature survey

Various literature survey and review works have been carried out.

b) Numerical modeling

Appropriate numerical modeling has been carried out.

c) Analytical studies

After analyzing the models using SAP 2000, the results have been studied systematically and interpretation of results has been carried out.

d) Discussion on results

Extensive discussions have been carried out on results.

e) Conclusion

Appropriate conclusions have been drawn on the significance of RC bands.

1.6 Organization of thesis

The thesis has been organized in eight chapters according as follows:

i. In chapter 1 introduction on subject matter of thesis has been presented and also discussion on present problems and issues, objective of study and methodologies adopted have been carried out.

ii. In chapter 2 literatures related to the proposed thesis works have been reviewed.

iii. In chapter 3 discussions has been carried out on numerical modeling.

iv. In chapter 4 analytical studies have been carried out.

v. In chapter 5 discussions on results has been carried out.

vi. In chapter 6 conclusion on the thesis work has been drawn.

vii. In chapter 7 recommendations regarding the problems has been stated.

viii. In Chapter 8 expected future works relating to this thesis work has been presented.

2. LITERATURE REVIEW

2.1 General

Dawe and Seah, Flanagan and Bennett **and** ***Angel et al.*** have investigated the out-of-plane response of infill panels subjected to horizontal loads in last years. They all have found that masonry panels restrained by a bounding frame can develop non-negligible out-of-plane resistance due to the formation of an arching mechanism and depending on the panel slenderness (height-to-thickness) ratio and the compressive strength of infill masonry.

Flanagan and Bennett also studied the influence of in-plane damage on out-of-plane capacity and they have concluded that the interaction of in-plane and out-of-plane responses is not generally significant from the load resistance standpoint: it seems to depend on the slenderness ratio and usually external infill panels are much less slender than internal ones. For high slenderness ratio infill, ***Angel et al.*** have experimentally found that the reduction of the out-of-plane strength due to in-plane damage could be as high as 50%.

McDowell et al and Dawe and Seah have developed analytical models to evaluate the out-of-plane arching action, respectively referring to a unidirectional (2D) and a bidirectional (3D) behavior of un-reinforced masonry slabs confined by rigid boundaries. Because of ***McDowell et al.*** model tendency to overestimate out-of-plane capacity, due to the assumed elastic perfectly plastic stress-strain relation and non considered interaction with in-plane damage, ***Angel et al.*** have proposed an improvement consisting in the introduction, into the ***McDowell et al.*** model scheme, of strength reduction factors that account for the influence of in-plane damage and the flexibility of the bounding frame. Starting from a simplification of their analytical model they also proposed a practical capacity assessment procedure. As reported by ***Shing and Mehrabi,*** both the models of ***Dawe and Seah*** and ***Angel et al.*** tend, in some cases, to overestimate the out-of-plane resistance.

A number of significant experimental tests have been performed on in-plane response of infill masonry panels bounded by RC frames under lateral loads. All studies have shown that the global response of infill wall bounded by RC frames is heavily influenced by the interaction of the infill with its bounding frame. The lateral capacity of infill wall bounded by RC frames usually depends on the interaction between the infill and the bounding frame: it can determine both the initial and the collapse mechanism. Under relatively low lateral loads the infill remains in contact with the frame structure and their contribution significantly increases the global stiffness of the frame. Under higher loads, the masonry infill, because of their no tension behavior partially separate from the bounding frame. This load resisting system can be classically represented as a frame with equivalent compression trusses as observed since early researches. Further collapse behavior can then evolve depending on relative strength and stiffness of frame structure and infill walls

Mehrabi et al. has demonstrated that relatively weak un-reinforced masonry infill can enhance the stiffness and strength of a non-ductile reinforced concrete frame significantly.

2.2 Characteristics of infill walls

2.2.1 Mode of failure

The following modes of failure are observed in infill walls:

i. Interface cracking

Such type of failure consists of separation of infill panel and the frame except at the compressive corners. This mode occurs at load magnitudes considerably below the ultimate. Up to the onset of interface cracking the system behaves elastically and monolithically similar to a composite plate.

ii. Diagonal cracking

This mode is characterized by a sudden crack through the wall, essentially on the compression diagonal.

iii. Corner crushing

This mode is usually accompanied by the formation of plastic hinge either in the column or in the beam.

iv. Out-of-Plane Failure

Ground shaking transverse to the plane of a wall may lead to an out-of-plane behavior mode. Experiments using air bags ***(Abrams, 1994)***, as well as shaking-table studies ***(Mander et al., 1994),*** show that for normal, infill panel, height-to-thickness ratios, considerable shaking is necessary to cause failure of the infill. However, out-of-plane failure may occur in the upper stories of high-rise buildings, where the floor accelerations are basically resonance amplifications of prominent sinusoidal ground motion input. In lower stories, when combined with high in-plane story shears, infill panels tend to progressively "walkout" of the frame enclosure on each cycle of loading. Although complete out-of-plane failure is not common, there is some evidence that this behavior mode has occurred. ***(FEMA 306, 1998)***

When the wall is slender and the direction of shaking is orthogonal to the plane of infill wall, the wall tends to topple (rocking). A crack in the wall is seen formed by shearing of masonry units in out-of-plane direction at the bed joint. The direction of crack is inclined; more or less along diagonal direction. The previously formed in-plane damage if any facilitates the failure in orthogonal direction.

2.2.2 Strength

The strength of infill wall is dependent on numerous parameters. Some of the important parameters are as follows:

i. Compressive strength of infill material

The strength is usually assumed proportional to the compressive strength of infill material.

ii. Relative stiffness parameter

The relative stiffness parameter denoted by λ_1 hereafter was studied by some investigators. This only affects the corner crushing strength.

iii. Height to length ratio

Height to length ratio has reducing effect on strength.

iv. Bending moment capacity of frame

Bending moment capacity of the frame has an enhancing effect on the strength.

v. Interface bond condition

Experimental and analytical investigations indicate that the interface shear bond does not influence the cracking strength markedly, but it increases the corner crushing strength.

vi. Lack of fit

For a small lack of fit of a few millimeters the ultimate strength is no significantly affected, where as the cracking strength is usually reduced.

2.2.3 Stiffness

Some influencing factors on stiffness are listed below:

i. Aspect ratio

Aspect ratio also known as height to length ratio of infill wall has effect on stiffness. As per experimental results of ***Benjamin and Williams*** and the analytical results of ***Riddington and Stafford-smith***, stiffness is almost constant for aspect ratios less than 0.5 and it decreases aspect ratios greater than 0.5.

ii. Mortar strength and curing

Mortar strength and curing has significant effects on stiffness.

iii. Lack of fit

Lack of fit greatly influences the stiffness, especially if the gap is located at the loaded corners.

2.3 Modeling techniques

Masonry modeling can be focused on macro-modeling of masonry as a composite or micro-modeling of the individual components, viz. unit (brick, block, etc) and mortar ***Rots (1991)***. The interface unit/mortar is responsible for most cracking as well as slip and can also be modeled. Depending on the level of accuracy and the simplicity desired, it is possible to use the following models. ***Fig-A5***

i. **Joints are represented by continuum elements**: In this approach, the mortar material between the blocks is represented by continuum elements, modeling phenomena resulting from different elastic properties of block and mortar.

ii. **Joints are represented by discontinuum elements**: This approach neglects the elastic properties of the mortar and associated local effects at the block-mortar interface, instead modeling the mortar joints as potential lines of failure due to cracking.

iii. **Joints are smeared out**. In this approach, the block-mortar composite is treated as a homogenous solid whose mechanical properties average the effects of the two interacting materials.

In the first approach, Young's modulus, Poisson's ratio and, optionally, inelastic properties of both unit and mortar are taken into account. In the second approach, mortar is smeared out in the interface element and in the unit. Due to the zero thickness of the interface elements, the geometry of the unit has to be expanded to

include the thickness of the joint. The third approach does not make a distinction between individual units and joints but treats masonry as an anisotropic composite

Page (1978) made the first attempt to use a micro-model for masonry structures. He modeled units as elastic continuum elements and the joints were modeled as linkage elements with nonlinear deformation characteristics. The elastic interface (σ, τ) - space was limited by the envelope obtained experimentally and shown in ***Fig-A6***. Here σ is the joint normal stress and τ is the joint shear stress. The yield surface of ***Fig-A6*** contains three different branches: one in tension and two in compression. The marked change in slope in compression corresponds to a change in the failure mode from pure shear failure in the joint to combined joint/unit failure. Non-linear behavior included brittle failure in tension and hardening in shear/compression. Hardening was simulated in a primitive way, assuming that the normal stiffness remains constant and the shear stiffness follows an experimental curve.

Arya and Hegemier (1978) proposed a different model for grouted masonry. A von Mises strain Softening model for compression with a tension cut-off was used for the units. Joints were modeled with interface elements with softening on both the cohesion and friction angle but a brittle tension cut-off.

Holmes (1961) was the first to suggest the equivalent diagonal strut. The infill wall is replaced by an equivalent compressive diagonal strut with an effective width ***'a'***. Though infill walls have a number of possible failure modes caused by the frame-infill interaction, equivalent strut models tentatively can be used to calculate the strength of an infill frame ***(FEMA 306, 1998)***. A dimensionless relative stiffness parameter was defined by ***Stafford Smith (1970)*** to determine the degree of frame-infill interaction and the effective width of the strut.

$$\lambda_1 = \left[\frac{E_{me} t_{inf} \sin 2\theta}{4 E_{fe} I_{col} h_{inf}} \right]^{1/4}$$

Effective width of equivalent strut, $a = 0.175 (\lambda_1 h_{col})^{-0.4} r_{inf}$ ***(FEMA 306, 1998) Fig-A7***

In which,

h_{col} = Column height between centerlines of beams (*mm)*

h_{inf} = Height of infill panel, (*mm)*;

E_{fe} = Expected modulus of elasticity of frame material (*MPa)*;

E_{me} = Expected modulus of elasticity of infill material (*MPa)*;

I_{col} = Moment of inertial of column (*mm4*);

L_{inf} = Length of infill panel (*mm)*;

r_{inf} = Diagonal length of infill panel (*mm)*;

t_{inf} = Thickness of infill panel and equivalent strut (mm *)*

θ = Angle whose tangent is the infill height-to-length aspect ratio (*radians)* given by the following:

$\theta = \tan^{-1}(h_{inf}/L_{inf})$

2.4 Material properties

G. Sarangapani, B.V. Venkatarama Reddy and K.S Jagadish (2002) had carried extensive experiment on behavior of mortar of different grades with different w/c ratio. Stress-strain relationships were obtained using cylinder specimens having 150 mm diameter and 305 mm height. Poisson's ratio was determined through prism size of 150 × 150 × 300 mm. The tests were carried out in compression testing machine. For mortar 1:6 with w/c ratio 0.8 the compressive stress-strain curve is shown below. ***Fig-A8***

R.H. Atkinson, G.R. Kingsley, S. Saeb, B. Amadei and S. Sture at University of Colorado had tested masonry specimens to find out the shear strength of brick masonry bed joints using direct shear apparatus. The test specimen was 152 mm wide and 440 mm long. A curve consisting of horizontal load versus relative horizontal displacement was plotted. ***Fig-A9***

Uma Shankar Shah (2002) in his M.Sc. thesis work carried different tests on machine made and local bricks in Nepal. Poisson's ratio of brick was determined by measuring lateral and longitudinal strain during test on UTM.

Poisson's ratio = Lateral strain/Longitudinal strain

Young's modulus of elasticity was determined using mathematical relationship between Young's modulus of elasticity, pulse velocity obtained from ultrasonic pulse velocity test and Poisson's ratio.

$$E = V^2 \times \rho \times (1+\nu) \times (1-2\nu) / (1-\nu)$$

Where,
E = Young's modulus of elasticity
ρ = Unit weight
ν = Poisson's ratio
V = Compressive wave velocity

Compressive strengths of bricks were tested on compressive strength testing machine. The compressive strength of brick was determined by dividing the total machine load by the contact area of the machine platen with the specimen at one side.

Tensile strength of brick was determined by flexure test under central point loading.

In a similar way compressive strength of brick masonry was found out by testing masonry prism on compressive testing machine.

2.4.1 Multi-Linear Kinematic Plasticity Property of link element

This model is based upon kinematic hardening behavior that is commonly observed in metals. For each deformational degree of freedom, multi-linear kinematic plasticity properties are specified. All internal deformations are independent. The deformation in one degree of freedom does not affect the behavior of any other. If nonlinear properties are not specified for a degree of freedom, that degree of freedom is linear using the effective stiffness, which may be zero. The nonlinear force-deformation relationship is given by a multi-linear curve that is defined by a set of points. The curve can take on almost any shape, with the following restrictions:

i. One point must be the origin, (0,0).

ii. At least one point with positive deformation, and one point with negative deformation, must be defined.
iii. The deformations of the specified points must increase monotonically, with no two values being equal.
iv. The forces (moments) at a point must have the same sign as the deformation (they can be zero).
v. The final slope at each end of the curve must not be negative.

The slope given by the last two points specified on the positive deformation axis is extrapolated to infinite positive deformation. Similarly, the slope given by the last two points specified on the negative deformation axis is extrapolated to infinite negative deformation.

The curve defines the force-deformation relationship under monotonic loading. The first slope on either side of the origin is elastic; the remaining segments define plastic deformation. If the deformation reverses, it follows the two elastic segments before beginning plastic deformation in the reverse direction.

Under the rules of kinematic hardening, plastic deformation in one direction "pulls" the curve for the other direction along with it. Matching pairs of points are linked. ***Fig-10***

2.5 Analysis techniques

Time-history analysis is a step-by-step analysis of the dynamical response of a structure to a specified loading that may vary with time. The analysis may be linear or nonlinear. Time-history analysis is used to determine the dynamic response of a structure to arbitrary loading. The dynamic equilibrium equations to be solved are given by:

$$\mathbf{M\ddot{u}}(t) + \mathbf{C\dot{u}}(t) + \mathbf{Ku}(t) = \mathbf{r}(t)$$

Where ***K*** is the stiffness matrix; ***C*** is the damping matrix; ***M*** is the diagonal mass matrix; **t** is the time function; **u**, **$\dot{\mathbf{u}}$**, and **$\ddot{\mathbf{u}}$** are the displacements, velocities, and

accelerations of the structure; and **r** is the applied load. If the load includes ground acceleration, the displacements, velocities, and accelerations are relative to this ground motion. Any number of time-history Analysis Cases can be defined. Each time-history case can differ in the load applied and in the type of analysis to be performed. There are several options that determine the type of time-history analysis to be performed:

a. **Linear vs. Nonlinear**: For linear system, the resisting forces are expressed in terms of entire values of velocity and displacement that have been developed in the structure up to that time. However, for nonlinear analysis it is assumed that the physical properties remain constant only for short increments of time or deformation.

b. **Modal vs. Direct-integration**: These are two different solution methods, each with advantages and disadvantages. Under ideal circumstances, both methods should yield the same results to a given problem.

If given a loading of known distribution in space and known variation with time, the resulting motion i.e. accelerations, velocities and displacements of degree of freedom as a function of time can be found out in different way using different methods.

In modal methods and related Ritz vector methods, the resulting motion can be found out by using an alternative (and reduced) set of degree of freedom, solving for these degree of freedoms as functions of time, then transforming back to the original physical degree of freedom.

As in any model analysis, the first step is to obtain the lower frequencies and modes of the structure by solving an undamped eigenproblem.

Let $\{\bar{u}\}_i$ be normalized with respect to the mass matrix; then,

If $\{\bar{u}\}_i^T [M] \{\bar{u}\}_i = 1$ then $\{\bar{u}\}_i^T [K] \{\bar{u}\}_i = \omega^2$

A *modal matrix* **[Φ]** is considered whose columns are the eigenvectors, normalized with respect to the mass matrix, and a diagonal spectral matrix **[ω²]** whose entries are the squared natural frequencies of vibration.

$$[\Phi] = [\bar{u}_1\ \bar{u}_2\ \bar{u}_3 \ldots\ldots\ldots\ldots \bar{u}_n] \qquad [\omega^2] = [\omega_1^2\ \omega_2^2\ \omega 3^2\ \ldots\ldots\ldots\ldots\ldots\ \omega_n^2]$$

Here *n* is the total number of degree of freedom not suppressed by boundary conditions or constraints.

It can be shown that $\{\bar{u}\}_i^T[M]\{\bar{u}\}_j = 0$ and $\{\bar{u}\}_i^T[K]\{\bar{u}\}_j = 0$, when $i \neq j$

$$[\Phi]^T[M][\Phi] = [I] \text{ and } [\Phi]^T[K][\Phi] = [\omega^2]$$

Where, **[I]** is a unit matrix. An arbitrary displacement vector **{u}** can be expressed as a linear combination of the eigenvectors; that is, as $\{u\} = \{\bar{u}\}_1 Y_1 + \{\bar{u}\}_2 Y_2 + \ldots\ldots\ldots + \{\bar{u}\}_n Y_n$. Thus

$$\{u\} = [\Phi]\{Y\} \quad \{\mathring{u}\} = [\Phi]\{\dot{Y}\} \quad \{\ddot{u}\} = [\Phi]\{\ddot{Y}\}$$

The Yi are generalized degree of freedom often called modal co-ordinates or modal displacements.

<u>In direct integration methods</u> the resulting motion can be found out by retaining the original degree of freedom and integrating the equations of motion using time increment **Δ**t. Direct integration refers to calculation of response history using step-by-step integration in time, without first changing the form of dynamic equations, as is necessary in modal methods. Response is evaluated at instants separated by time increment **Δ**t, so we compute structure displacements at times **Δ**t, 2 **Δ**t, 3 **Δ**t, …….,n **Δ**t, and so on. At the *n*th time step, the equation of motion is:

$$M\{\ddot{u}(t)\}_n + C\{\mathring{u}(t)\}_n + K\{u(t)\}_n = \{r(t)\}_n$$

In non-linear problem **[K]** may change from one time step to the next.

Discretization in time is accomplished by using finite difference approximations of time derivatives. Method of direct integration calculate conditions at time step n + 1

from the equation of motion, a difference expression, and known conditions at one or more preceding time steps. Algorithms can be classified as explicit or implicit. An explicit algorithm uses a difference expression of the general form:

$\mathbf{\{u\}_{n+1} = f\,[\{u\}_n, \{\dot{u}\}_n, \{\ddot{u}\}_n, \{u\}_{n-1}, \ldots\ldots]}$, which contains only historical information on its right-hand side. An implicit algorithm uses a difference expression of the general form:

$\mathbf{\{u\}_{n+1} = f\,[\{\dot{u}\}_{n+1}, \{\ddot{u}\}_{n+1}, \{u\}_n, \{\dot{u}\}_n, \{\ddot{u}\}_n, \ldots\ldots]}$, which is combined with the equation of motion at time step n + 1.

The important differences between explicit and implicit methods are related to stability and economy. Explicit methods are *conditionally stable*, which means there is a critical time step $\mathbf{\Delta}t_{cr}$ that must not be exceeded if the numerical process is not to "blow up" by becoming unstable. Because $\mathbf{\Delta}t_{cr}$ is quite small, a great time many time steps are needed, but each is executed quickly. Commonly used implicit methods are *unconditionally stable*, which means that calculation remain stable regardless of how large $\mathbf{\Delta}t$ becomes. In explicit methods, the coefficient matrix of $\{u\}_{n+1}$ can be made diagonal, so that $\{u\}_{n+1}$ is cheaply calculated in each time step. In implicit methods, the coefficient matrix {u}n+1 can not be made diagonal, so that cost per unit time step is greater, increasingly so as the finite element mesh increases in dimensionality.

In direct integration time history analysis the explicit method can be used at low cost per time step but many steps required and the implicit method can be used at higher cost per time step but few steps required.

Following points are to be considered to make appropriate choice among the different methods of time history analysis.

i. The modal method is suited to structural dynamics problems. Major expense of this method is in solving the eigenvectors, so efficiency is greatest when very few modes are needed.
ii. Implicit direct integration is suited to structural dynamics problems. It competes with the modal method, and may be cheaper where many modes

would be needed in the modal method and when the analysis need not span as great a time. Cost per unit time is substantial in 2D and 3D problems, but, in contrast with explicit direct integration method, the size of **Δ**t is limited by considerations of accuracy rather than numerical stability. The main advantage of implicit direct integration method is that vibration frequencies and modes need not be computed.

iii. Explicit direct integration is best suited to wave propagation problems. Cost per time step is small, but so is the critical time step, so the method is not well suited to structural dynamics problems. Nonlinearity can be accommodated with relative ease.

Direct integration results are extremely sensitive to time-step size in a way that is not true for modal superposition. Direct-integration analyses should always be run with decreasing time-step sizes until the step size is small enough that results are no longer affected by it.

Since a variety of common methods are available for performing direct-integration time-history analysis, the default "Hilber-Hughes-Taylor alpha" (HHT) method had been used on the analysis of this thesis work. The HHT method uses a single parameter called alpha. This parameter may take values between 0 and -1/3. For alpha = 0, the method is equivalent to the Newmark method with gamma = 0.5 and beta = 0.25, which is the same as the average acceleration method (also called the trapezoidal rule.) Using alpha = 0 offers the highest accuracy of the available methods, but may permit excessive vibrations in the higher frequency modes, i.e., those modes with periods of the same order as or less than the time-step size. For more negative values of alpha, the higher frequency modes are more severely damped. This is not physical damping, since it decreases as smaller time-steps are used. However, it is often necessary to use a negative value of alpha to encourage a nonlinear solution to converge. For best results, the smallest time step is used as practicable as possible and alpha is selected as close to zero as possible.

c. **Transient vs. Periodic**: Transient analysis considers the applied load as a one-time event, with a beginning and end. Periodic analysis considers the load to repeat indefinitely, with all transient response damped out.

3. NUMERICAL MODELING

3.1 Geometrical configuration

i. A three dimensional RC framed building with number of bays, bays width, number of stories and storey height within the limitation specified on ***Nepal National Building Code (NBC 201: 1994)*** as thumb rule (common residential building).
ii. Number of stories = 3 (Limitation = 3)
iii. Number of bays = 3 with 4 m bay width in X-direction and 2 with 4 m bay width in Y-direction (Limitation = 6 bays or maximum 25 m length in each direction, bay width limitation = 4.5 m)
iv. Storey height = 3 m (Limitation = Total height of building 11 m)
v. Column = 230×230 mm
vi. Beam = 230×300 mm
vii. Infill wall = ½ brick wall ; 10 mm thick mortar

Limiting configuration of building to apply thumb rule given in ***(NBC 201:1994)*** is given in ***fig-A11.*** To select the building for modeling, this configuration was taken as reference.

3.2 Assigning material properties

a) Bricks:

Size: 240 mm × 115 mm × 57 mm ***Nepal Standard Brick Masonry NS: 1/2035 [22]***

Density =1710 Kg/m^3 (Local bricks)
Poisson's ratio (ν) = 0.11
Modulus of Elasticity (E) = 2775 N/mm²
Compressive strength (σ) = 24 N/mm²
Tensile strength = 3.69 N/mm²

b) Masonry

Infill masonry = Local brick masonry in 1:6

Compressive strength of masonry prism (f_m) = 2.38 N/mm²

Uma Shankar Shah, M.SC. Thesis (2002)

c) Mortar

i. Cement sand mixes of 1:6 (Commonly adopted in general construction) ***NBC: 201, cl.5.1***

ii. Stress-strain curve developed by ***G. Sarangapani, B.V. Venkatarama Reddy and K.S. Jagadish (Indian Institute of Science Banglore)*** were taken for compressive strength of the mortar.

iii. This stress strain curve in literature was approximated by converting it to a multi linear curve. ***Fig-A12***

iv. Curve developed by ***R.H. Atkinson, G.R. Kingsley, S. Saeb, B. Amadei and S. Sture at University of Colorado*** was taken for shear strength of mortar.

v. This force displacement curve which is actually a multi linear one was also approximated to simplified multi linear curve.

vi. This force displacement curve was converted into stress strain curve considering the shearing area of the test specimen. ***Fig-A13***

vii. Such stress strain curves were converted to force displacement curves using tributary area and thickness of mortar at different locations so as to find the stiffness of the non-linear springs. The mortar at different locations had different force displacement curves since the tributary area were different at different locations.

c) Concrete

Grade = M20

(Minimum grade of concrete specified by *IS 456:2000*)

$E_c = E_{fe} = 5000 \sqrt{f_{ck}}$ ***IS 456:2000***

Shear strength of RCC (τ_{max}) = 2.7 N/mm²

(Calculated using the detailing given in *NBC: 2001* as per *IS 456:2000*)

3.3 Modeling of different components

Micro modeling was carried out for the focused infill panel of the building and approximate modeling was carried out for other panels. The modeling features are as follows:

i. The bricks were modeled as 8-noded rectangular solid element. Each brick is divided into three solid elements.
ii. The mortar was represented by non-linear (Kinematics) springs that connect adjacent units at nodes. ***Fig-A14***
iii. To take into account the sliding of units in orthogonal direction (i.e. to account bond shear failure), spring elements are added which connect nodes of same units in orthogonal direction.
iv. The surrounding columns and beams were modeled as solid elements with sufficient sub-divisions so that the nearby bricks can be connected by springs at corresponding nodes. ***Fig-A15 and A16***
v. Except the beams and columns of bounding frame of concerned panel, all other frames (Beams and columns) are modeled roughly with three dimensional single solid elements. ***Fig-A17***
vi. Expect the infill panel of interest; all other infill panels were modeled by equivalent strut so as to account the stiffness of other infill panels. ***Fig-A18***
vii. The connection between equivalent strut and beam column junction was made using gap element.

Width of equivalent strut

$E_{me} = 750\times f_m$ ***Paulay and Priestely (1992)***

$= 750\times 2.38 = 1785$ N/m²

$t_{inf} = 115$ mm

$E_{fe} = 5000\times (20)^{0.5} = 22361$ N/mm²

$h_{inf} = 2700$ mm

$L_{inf} = 3770$ mm

$r_{inf} = [2700^2 + 3770^2]^{0.5} = 4637$ mm

h_{col} = 3000 mm

$\theta = \tan^{-1}(2.7/3.77) = 35.61^{\circ}$

$I_{col} = 230 \times 230^3/12 = 233.2 \times 10^6$ mm^4

$\lambda_1 = [(1785 \times 115 \times \text{Sin}71.22^{\circ})/ (4 \times 22361 \times 233.2 \times 10^6 \times 3770)]^{0.25} = 0.001254$

$a = 0.175 \times (0.001254 \times 3000)^{-0.4} \times 4637 = 477.65$ mm $\approx$ 480 mm

Hence width of diagonal strut = 480 mm

The infill walls expect the concerned panel were modeled using equivalent strut of width 480 mm and thickness equal to thickness of infill wall i.e. 115 mm.

4. ANALYTICAL STUDIES

4.1 General

After modeling the wall non-linear direct integration time history analysis was carried out for both type of infill walls (with and without RC bands) using software SAP 2000 taking a famous earthquake El Centro. The time step taken was 0.005 sec.

Since the analysis has been carried out at time step 0.005 sec, there is huge volume of out put data for each step and the number of steps during complete analysis is very large. So to deal with data of each step and carry out comparative study is very difficult. So the output data of the time period at which response is largest was found out. The time is t = 2.02 Sec. Then the results for that particular step was analyzed and compared.

4.2 Stresses in bricks

Since the output contains huge volume of data, dealing with the stresses of each masonry unit is very difficult. So the maximum stressed masonry unit during entire loading history was found out and dealt with that masonry unit to find the stress history for comparative study. The masonry units having maximum six different types of stresses may be different.

During entire loading period, six different stress components (S11, S12, S13, S22, S23, and S33) were considered and the brick elements which has maximum such stresses were identified. Then the stress histories of corresponding brick elements were plotted and studied. For example, during entire loading period, the brick element which has maximum normal stress (S11) was identified and for that brick element, the normal stress (S11) history was plotted. Similarly during entire loading period, the brick element which has maximum shear stress (S12) was identified and the shear stress (S12) history for that brick element was plotted. This process was repeated for all other types of stresses. This process of studying the different stress histories was

carried out for both types of models i.e. with and without bands. Then the stress histories of two models were studied and compared.

4.3 Displacement of bricks

During entire loading period, the brick elements which has maximum displacement from its original position in X or Y direction (i.e. in-plane or out-of-plane) was identified and for that particular brick element, the displacement history was plotted and studied. For example, brick element which has maximum displacement in X-direction (in-plane direction) during entire loading period was identified and for that brick element, the displacement history was plotted. Similarly, the brick element which has maximum displacement in Y-direction (out-of-plane direction) was identified and the corresponding displacement history was plotted. While calculating displacement of brick element, the mean displacement of all eight nodes was taken. The displacement history was plotted for both type of models and the results were studied and compared.

During entire loading, the time at which the displacements on bricks have maximum value was found out. The time was t = 2.02 sec. For that particular time period, the displacements of bricks along the height of wall were found at different locations i.e. at left most portion of wall which consist the bricks at the vicinity of left column, at middle portion of wall, and at right portion of wall which consist bricks at the vicinity of right column. The displacement of bricks with height was plotted with respect to height of wall at different locations. This job was carried out for both models. The results of two models were studied and compared.

4.4 Crack patterns in infill walls

The time at which the force in the spring element provided has maximum was found out. The spring force was maximum at time t = 2.02 Sec. At time t = 2.02 Sec., the forces on all springs were found out. Those spring forces were converted into stresses using corresponding tributary areas.

Failure criteria of the mortar were fixed taking into account the maximum stress in stress-strain curve. Those elements which have stress greater or equal to the maximum stress i.e. greater or equal to 100 % of maximum stress, greater or equal to 80 % and less than 100 % of the maximum stress and greater or equal to 60 % and less than 80 % of the maximum stress were identified and all other elements were discarded. The nodes containing the springs which contains above mentioned value of stresses were joined by smooth lines and hence cracking pattern was plotted. The stresses on the bricks were also studied to know whether any of the bricks were crushed or not. This task was carried out for both types of models. The results obtained were studied and conclusion was drawn.

4.5 Effect of RC bands on bounding frames

At time t = 2.02 Sec., at which stresses on frames were maximum, the different stresses (S11, S12, S13, S22, S23 and S33) were found out on the different solid elements of the bounding frames i.e. left column, right column, bottom beam and top beam. For columns, height (X-axis) versus maximum stress (Y-axis) was plotted for both types of models and the results were compared. For beams distance from left beam column junction (X-axis) versus maximum stress (Y-axis) was plotted for two models and the results were studied.

5 RESULTS AND DISCUSSIONS

5.1 Stresses on bricks

During entire loading period, different type of stresses attain their highest values at time t = 2.02 sec. The bricks which have highest stresses (S11, S12, S13, S22, S23, and S33) during entire loading history on whole model were identified and for those individual bricks, the corresponding stresses were plotted with respect to time to see the entire stress history. This job was carried out for both types of models i.e. with and without band. Plotting of stresses with respect to time compares nearly with the input acceleration history for both models. It is noticed that no brick units attain the stresses greater or equal to failure stress.

During entire loading history, though the normal stresses (S11) at different time for model having band has less values in comparison with the corresponding values for model without band, the difference is not much significant. The maximum normal stress (S11 = 141.16 KN/m²) for wall with band is approximately 7 % less than the maximum normal stress (S11 = 150.61 KN/m²) for wall without band. This result indicates that the role of RC bands for in-plane action is not much significant. ***Fig-B1***

While comparing shear stress (S12) for two models at different time, it is seen that the maximum shear stress (S12 = -106.28 KN/m²) for wall with band is approximately 49 % less than the maximum shear stress (S12 = -158.62 KN/m²) for wall without band. This difference is significant one and we can conclude that the role of RC band for out of plane shear stress is much significant. ***Fig-B2***

Comparison of shear stress (S13) indicates that the maximum shear stress (S13 = 185.54 KN/m²) for wall with band is approximately 34 % less than the maximum shear stress (S13 = 249.15 KN/m²) for wall without band. ***Fig-B3***

The normal stresses (S22) for two models are almost same. The maximum normal stress (S22 = -39.83 KN/m²) for model with band is only approximately 4 % less than

the maximum normal stress (S22 = -41.42 KN/m²) for model without band. Also the magnitude of normal stress (S22) during entire loading is less than other types of stresses. ***Fig-B4***

While observing the variation of shear stress (S23) with time it is found that the maximum shear stress (S23 = 151.2 KN/m²) for model with band is approximately 33 % less than the maximum shear stress (S23 = 200.16 kN/m²) for model without band. ***Fig-B5***

The maximum normal stress (S33 = 242.52 KN/m²) for model with band is approximately 12 % less in comparison with the normal stress (S33 = 272.51 KN/m²) for model with out band. ***Fig-B6***

From the above discussion we can conclude that the different types of maximum stresses in wall with band are always less than the wall without band. The difference in shear stress is much higher than the difference in normal stresses. The reason behind the less value of stresses for model with band may be due to the fact that the presence of band makes the building stiffer in comparison with that in absence of band. This fact is reflected on the result of maximum displacement of building as shown in ***Fig- B7 and B8.*** The result shows that the maximum displacement of building with band (U1 = 0.001388 m and U2 = 0.001054 m) is approximately U1 = 35 % less and U2 = 39 % less in comparison with the maximum displacement of building without band (U1 = 0.001867 m and U2 = 0.002096 m).

5.2 Displacements of bricks

During entire period of loading, the brick having maximum displacement in X and Y direction (at time t = 2.02 sec) was identified and the displacement of that brick with time was studied for both type of models. The displacement history of brick with time is approximately similar to the history of input acceleration.

While comparing the displacement of brick in X-direction, it is seen that the difference in maximum displacement of brick in two models is not much significant. The maximum displacement of brick for model with band (U1 = 0.001249 m) is

approximately 4 % less than the maximum displacement of brick for model without band (U1 = 0.001299 m). ***Fig-B9***

However in Y-direction, the difference in maximum displacement of brick in two models is significant. The maximum displacement of brick for model with band (U2 = 0.001363 m) is approximately 24 % less than the maximum displacement of brick for model without band (U2 = 0.001691 m). ***Fig-B10***

Maximum displacement of bricks (at time t = 2.02 sec) were found at left end, mid portion and right end of infill wall and displacement was plotted with respect to height of wall for both types of models. It is found that the displacement of brick element increases with height linearly for both models.

While observing the in-plane displacement of bricks, the difference in in-plane displacement for two models is not significant. The maximum in-plane displacement of brick at left end of infill wall with band (U1 = 0.001244 m) is approximately 4 % less than the maximum in-plane displacement of brick at left end of infill wall without band (U1 = 0.001298 m). Similarly the maximum in-plane displacement of brick at mid height for wall with band (U1 = 0.001242 m) is approximately 4 % less in comparison with the wall without band (U1 = 0.001295 m). The maximum in-plane displacement for wall with band at right corner (U1 = 0.001252 m) is also approximately 4 % less in comparison with the maximum in-plane displacement of bricks in wall without band at right corner (U1 = 0.001302 m). ***Fig-B11, B12 and B13***

But the difference in maximum out-of-plane displacement of bricks for two models is significant. The maximum out-of-plane displacement of brick at left end of wall with band (U2 = 0.001367 m) is approximately 24 % less than the maximum out-of-plane displacement of brick at left end of wall without band (U2 = 0.001699 m). Similarly the maximum out of plane displacement of brick at mid of wall for model with band (U2 = 0.001308 m) is approximately 21 % less in comparison with the maximum displacement of brick at mid height of wall for model without band (U2 = 0.001578 m). The maximum out-of-plane displacement of brick at right end of wall with band (U2 = 0.001367 m) is approximately 17 % less than the maximum out-of-plane

displacement of brick at right end of wall for model without band (U2 = 0.001599 m). ***Fig-B14, B15 and B16***

From above stated facts we can conclude that since the maximum out-of-plane displacement of brick for model with band is significantly less than the maximum out-plane-of displacement of brick for model without band, the presence of RC band in infill masonry wall is very effective in preventing out-of-plane failure of wall. The presence of band has also reduced the maximum in-plane displacement of brick though the difference is not much significant. The reason is due to the fact that the in-plane stiffness of wall increases due to presence of band and hence the displacement is low. It is also seen that the maximum displacement of brick is more at right and left end than the maximum displacement of brick at mid of wall which indicates the failure is tending toward the separation of wall and the bounding column.

5.3 Crack patterns in infill walls

The maximum forces on the spring element of the model was found out at (time t = 2.02 sec). The spring force was converted to corresponding to stress using tributary area so as to find the stress on mortar. The failure shear and compressive stress were taken equal to maximum shear (0.26 N/m^2) and maximum compressive (3.2 N/m^2) stresses as indicated in stress-strain curves. ***Fig.A12 and A13***

The spring element having forces corresponding to stress equal to 60-79 %, 80-99 % and equal to greater than 100 % of failure stress were grouped and other springs were not accounted. The path of the stress corresponding to above mentioned groups were plotted manually and the path of crack propagation was found out for both types of model. ***Fig-B17 and B18***

The crack pattern shown in figure implies that the wall without band is tending to fail after forming approximately diagonal crack. The wall is near to collapse condition. Near corner of the wall severe damages have been observed. Both types of failure (in-plane and out-of-plane) of mortar have been observed in topmost corners and in-plane failure of mortar has been observed near bottom corners. Since the direction of input earthquake acceleration was in X and Y direction, the effect of corner crushing has

been clearly seen which is mainly due to in-plane seismic shock. The damage on the lower most corner is only due to in-plane action and on the top corner is due to in-plane as well as out-of-plane action. Expect on corners all the other springs are failed on shear i.e. out-of-plane failure only. The junction between wall and bounding column has failed on upper part of the wall and on the lower part of the wall the junction is tending to fail. The junction between beam and column on upper part has separated due to failure of mortar in shear but the bottom junction of beam and wall has been separated near corners only which may be the effect of in plane action. The wall with out band has almost fallen out.

But the damage in wall with band is not much significant in comparison to the wall without band. Minor corner crushing has also been observed in the wall with band but not as much as the wall without band. The crack on the wall tends to propagate along diagonal direction but the RC band does not allow propagating. The tendency of mortar toward out of plane shear failure seems clearly but the failure has not occurred yet. The RC band behaves as if it is a beam. So symptom of corner crushing seems clearly. Though trend of failure is likely to occur similar to the wall without band provided that the RC bands have also played the role of beam, the damage in the wall is very less than the wall without band.

From the above stated discussion we can conclude that the RC band has significant role in preventing the failure of the wall. In-plane action of the seismic shock has approximately same impact on two models but out-of-plane action of seismic shock has significantly less impact on the wall with band than the wall without band. The wall without band has almost collapsed but the damage on the wall with band is repairable one.

5.4 Effect of RC bands on bounding frames

Left column

All types of normal stresses are very high near the junction of beam column than at other regions. There is stress concentration (sudden jerking on stress pattern) though smaller in magnitude than at beam column junction for the wall with band at band

column junction. This is due to the fact that the RC band is acting as if it is a small beam.

The maximum normal stress along the column (S11 = 800.11 KN/m²) for wall with band is approximately 12 % less in comparison with the wall with out band (S11 = 898.14 KN/m²). At all locations the stress for wall with band is less than the stress for wall without band expect at band column junction where sudden change in stress pattern has been observed. ***Fig-B19***

The maximum shear stress along the column (S12 = -376.13 KN/m²) for wall with band is approximately 8 % less in comparison with the wall with out band (S12 = -405.48 KN/m²). At all locations the stress for wall with band is less than the stress for wall without band expect at band column junction where sudden change in stress pattern has been observed. ***Fig-B20***

The maximum shear stress along the column (S13 = -668.27 KN/m²) for wall with band has no significant difference than the corresponding stress for the wall without band. At all locations the stress for wall with band is less than the stress for wall without band expect within approximately lower one third height where slightly high stress for model with band has been observed and at band column junction where has increased suddenly. ***Fig-B21***

The maximum normal stress along the column (S22 = -1159.33 KN/m²) for wall with band is approximately 9 % less in comparison with the wall with out band (S22 = -1266.12 KN/m²). At all locations the stress for wall with band is less than the stress for wall without band expect at band column junction where sudden change in stress pattern has been observed. ***Fig-B22***

The maximum shear stress along the column (S23 = -889.23 KN/m²) for wall with band has no significant difference than the corresponding stress for the wall without band. At all locations the stress for wall with band is less than the stress for wall without band. At band column junction sudden change in stress pattern has been observed. ***Fig-B23***

The maximum normal stress along the column (S33 = 1984.8 KN/m²) for wall with band is approximately 15 % less in comparison with the wall with out band (S33 = 2283.99 KN/m²). At all locations the stress for wall with band is less than the stress for wall without band expect approximately at lower half height where normal stress (S33) for wall with band is slightly more than the wall without band and at band column junction where sudden change in stress pattern has been observed. ***Fig-B24***

Right column

The maximum normal stress along the column (S11 = -718.53 KN/m²) for wall with band is approximately 9 % less in comparison with the wall with out band (S11 = -780.83 KN/m²). At all locations the stress for wall with band is less than the stress for wall without band expect at band column junction where sudden change in stress pattern has been observed. ***Fig-B25***

The maximum shear stress along the column (S12 = 492.31 KN/m²) for wall with band is approximately 4 % less in comparison with the wall with out band (S12 = 511.03 KN/m²). At all locations the stress for wall with band is less than the stress for wall without band expect at band column junction where sudden change in stress pattern has been observed. ***Fig-B26***

The maximum shear stress along the column (S13 = -820.38 KN/m²) for wall with band has no significant difference than the corresponding stress for the wall without band. At all locations the stress for wall with band is less than the stress for wall without band expect within approximately upper one third height where slightly high stress for model with band has been observed and at band column junction where has increased suddenly. ***Fig-B27***

The maximum normal stress along the column (S22 = -2254.56 KN/m²) for wall with band is approximately 9 % less in comparison with the wall with out band (S22 = -2459.05 KN/m²). At all locations the stress for wall with band is less than the stress for wall without band expect at band column junction where sudden change in stress pattern has been observed. ***Fig-B28***

The maximum shear stress along the column (S23 = -1395.15 KN/m²) for wall with band has no significant difference than the corresponding stress for the wall without band. At all locations the stress for wall with band is less than the stress for wall without band. At band column junction sudden change in stress pattern has been observed. ***Fig-B29***

The maximum normal stress along the column (S33 = -2696.72 KN/m²) for wall with band is approximately 2 % less in comparison with the wall with out band (S33 = -2757.38 KN/m²). At all locations the stress for wall with band is less than the stress for wall without band expect approximately at upper one third height where normal stress (S33) for wall with band is slightly more than the wall without band and at band column junction where sudden change in stress pattern has been observed. ***Fig-B30***

Lower beam

The maximum normal stress along the beam (S11 = 3665.94 KN/m²) for wall with band is approximately 9 % less in comparison with the wall with out band (S11 = 4329.73 KN/m²). At all locations the stress for wall with band is less than the stress for wall without band. ***Fig-B31***

The maximum shear stress along the beam (S12 = 2240.38 KN/m²) for wall with band is approximately 5 % less in comparison with the wall with out band (S12 = 2360.15 KN/m²). At all locations the stress for wall with band is less than the stress for wall without band. ***Fig-B32***

The maximum shear stress along the beam (S13 = 3237.30 KN/m²) for wall with band has no significant difference than the corresponding stress for the wall without band. Here the beam has failed in shear. At all locations the stress for wall with band is approximately equal to the stress for wall without band ***Fig-B33***

The maximum normal stress along the beam (S22 = -2057.98 KN/m²) for wall with band is approximately 9 % less in comparison with the wall with out band (S22 = -

2212.67 KN/m²). At all locations the stress for wall with band is less than the stress for wall without band. ***Fig-B34***

The maximum shear stress along the beam (S23 = -935.23 KN/m²) for wall with band has no significant difference than the corresponding stress for the wall without band. At all locations the stress for wall with band is approximately equal to the stress for wall without band ***Fig-B35***

The maximum shear stress along the beam (S33 = -2634.12 KN/m²) for wall with band has no significant difference than the corresponding stress for the wall without band. At all locations the stress for wall with band is approximately equal to the stress for wall without band. ***Fig-B36***

Top beam

The maximum normal stress along the beam (S11 = 1030.30 KN/m²) for wall with band is approximately 10 % less in comparison with the wall with out band (S11 = 1130.22 KN/m²). At all locations the stress for wall with band is less than the stress for wall without band. ***Fig-B37***

The maximum shear stress along the beam (S12 = 737.22 KN/m²) for wall with band is approximately 4 % less in comparison with the wall with out band (S12 = 765.16 KN/m²). At all locations the stress for wall with band is less than the stress for wall without band. ***Fig-B38***

The maximum shear stress along the beam (S13 = -376.91 KN/m²) for wall with band is approximately 3 % less in comparison with the wall with out band (S13 = -387.53 KN/m²). At all locations the stress for wall with band is less than the stress for wall without band. ***Fig-B39***

The maximum normal stress along the beam (S22 = 823.76 KN/m²) for wall with band is approximately 5 % less in comparison with the wall with out band (S22 = 867.56 KN/m²). At all locations the stress for wall with band is less than the stress for wall without band. ***Fig-B40***

The maximum normal stress along the beam (S23 = -105.60 KN/m²) for wall with band is approximately 2 % less in comparison with the wall with out band (S23 = -107.46 KN/m²). At all locations the stress for wall with band is less than the stress for wall without band. ***Fig-B41***

The maximum shear stress along the beam (S33 = 320.74 KN/m²) for wall with band is approximately 12 % less in comparison with the wall with out band (S33 = 358.00 KN/m²). At all locations the stress for wall with band is less than the stress for wall without band. ***Fig-B4***

6 CONCLUSIONS

i. The building with wall having RC bands is stiffer than the building with wall without RC bands. So the deflection of building as a whole is less for the model with RC bands.

ii. Maximum stresses on the brick units for the wall with RC bands is less than the stresses on the wall without RC bands. In comparison to the in-plane stresses, the out-of-plane stresses are significantly less for the wall with RC bands. So provision of RC bands has large contribution to the phenomenon of preventing the failure of infill wall, especially in out-of-plane direction.

iii. Also the maximum displacement of masonry units for the wall with RC bands is less than the maximum displacements of masonry units for the wall without RC bands. Especially the out-of-plane displacement is significantly small for the wall with RC bands. This also proves the contribution of RC bands in preventing the failure of infill walls, particularly in orthogonal direction.

iv. Due the presence of RC bands, the wall with RC bands has fewer cracks than the wall without RC bands. The cracks tend to propagate diagonally from the beam column junction. The cracks on the corners are significantly large due the corner crushing effect of in-plane action. The in-plane damage facilitates the out-of-plane damage to occur rapidly. For the models studied, the wall with band is near to collapse but the damage on the wall with band is repairable.

v. The RC band behaves as if it is a beam connected to the column.

vi. The effect of RC bands on column is notable. The maximum stresses on the column occur always on beam column junction and those stresses for the wall with band are less than the corresponding stresses for the wall with out RC bands. But at the band column junction, due to the behavior of band like

beam the stresses for the wall with band are higher than the stresses for the wall without beam though the magnitude is small. The discontinuity on the variation of stresses especially in out-of-plane shear is clearly seen at the band column junction. If such condition occurs during large seismic shaking, there are every chances of failure of column at band column junction also.

vii. The effect of RC bands for the stresses on beam is not much significant though the stresses for the wall with RC bands are slightly less than the stresses for the wall without band.

viii. In summary the provision of RC band is very much beneficial to prevent the out-of-plane failure of infill masonry walls.

7 RECOMMENDATIONS

i. On the light of above discussed facts since the RC bands are beneficial in preventing the out-of-plane failure of infill masonry wall, the RC bands should be provided on infill walls especially in low rise buildings where brick masonry walls are used as infill walls like in our country Nepal.

ii. The RC bands should be treated as beams and in a similar manner to beam column junction, the confined shear reinforcement should be provided at band column junction. This matter is not stated in NBC code in generalized form. But for the particular structures confined by certain criteria mentioned on NBC code, the thumb rule specified on code may be good because it specifies the ductile detailing.

iii. Due care should be given in designing column for the infill wall with RC bands than the beams.

8 WORKS FOR FUTURE

i. The same job can be carried out at other different storey also and the effect of storey on the results can be seen.

ii. The same task can be done for wall with openings. The contribution of RC band on infill wall with opening can be found out.

iii. Experimental investigation of the same task can be carried out. An appropriate shaking table test can be carried out to have confidence on the numerical results.

References

1. Nepal National Building Code: **(NBC 201:1994)**

2. Journal of Structural Engineering: **Vol. 118, no. 9, September, 1992**

3. Journal of Structural Engineering: **Vol. 121, no. 11, November, 1995**

4. Journal of Structural Engineering: **Vol.30, April-June 2003**

5. Journal of Structural Engineering: **Vol. 126, no. 9, September, 2000**

6. Journal of Structural Engineering: **Vol. 127, no. 1, January, 2001**

7. Journal of Structural Engineering: **Vol. 123, no. 5, May, 1997**

8. **FEMA 273/1997**: NEHRP Guidelines for the Seismic Rehabilitation of Buildings

9. **FEMA 302/1997**: NEHRP Recommended Provisions for Seismic Regulations for New Buildings and Other Structures

10. **FEMA 306/1998**: Evaluation of Earthquake Damaged Concrete and Masonry Wall Building

11. **FEMA 308/1998**: Repair of Earthquake Damaged Concrete and Masonry Wall Buildings

12. **FEMA 356/2000:** Pre-standard and Commentary for the Seismic Rehabilitation of Buildings

13. **Computers and Structures, Inc. 1995 University Avenue Berkeley, California 94704 USA**: SAP2000 Analysis Reference Manual

14. **Orton Andrew**: Structural design of masonry

15. **Cook D. Robert, Malkus S. David, Plesha E. Michael and Witt J. Robert**: Concept and Application of Finite Element Analysis

16. **Chopra K. Anil** : Dynamics of Structures Theory and Application to Earthquake Engineering

17. **Clough W. Ray, Penzien Joseph** : Dynamics of Structures

18. **IITK –BMTPC** Earthquake Tips

19. **Curtin W.G., Shaw G., Beck J.K., Bray W.A.**: Structural masonry designer's manual

20. **Mosalam Khalid M., White Richard N. and Gergely Peter**: Seismic Evaluation of Frames with Infill Walls Using Quasi-static Experiments

21. **Moghaddam Hassan A and Dowling Patrick J, Civil Engineering Department Imperial College, London**: Earthquake Resistant Design of Brick Infilled frames

22. **Prof. Dr. Mann W., Prof. Dr. König G. and Dr. ötes A., Technical University Darmstadt, Federal Republic of Germany**: Tests of Masonry Walls Subjected to Earthquake Forces

23. **Ghobarah and Mandooh K.EI, Hamilton ON University, Canada**: Out of plane strengthening of un-reinforced masonry walls with opening

24. **Langenbach Randolph**: Armature Crosswall Project

25. **Thürlimann B. and Guggisberg R., Institute of Structural Engineering, Swiss Federal Institute of Technology, Switzerland:** Failure Criterion for Laterally Loaded Masonry Walls: Experimental Investigation

26. **Shing P. Benson; University of Colorado, USA and Mehrabi Armin B.; Construction Technology Laboratories, USA**: Behavior and analysis of masonry-infill frames

27. **Lee Han-Seon and Woo Sung-Woo; Korea University, Korea**: Effect of masonry infill on seismic performance of a 3-storey R/C frame with non-seismic detailing

28. **Jagdish K.S., Professor, Department of Civil Engineering, IISC, Banglore**: Masonry building subjected to earthquake ground motions

29. **Zarnic Roko, Gostic Samo, Crewe J. Adam and Taylor A. Colin**: Shaking table tests 1:4 reduced scale models of masonry infill reinforced concrete frame buildings

30. **Mostafaei Hossein and Kabeyasawa Toshimi, Earthquake Research Institute, the University of Tokyo**: Effect of infill masonry walls on the seismic response of reinforced concrete building subjected to the, - Bam Earthquake Strong Motion: A Case Study of Bam Telephone Center

31. **Lourenço P. B., Delft University of Technology Faculty of Civil Engineering:** Analysis of masonry structures with interface elements

32. **Galati Nestore, Garbin Enrico, Tumialan Gustavo, and Nanni Antonio:** Design guidelines for masonry structures: Out of plane loads

33. **Athanasios D. Tzamtzis; Technological Educational Institute of Athens, Greece:** Finite Element Modeling of Cracks and Joints in Discontinuous Structural Systems

34. **Calvi G. Michele, Bolognini Davide, Penna Andrea; University of Pavia, Italy;:** Seismic Performance of Masonry-Infill RC Frames: Benefits of Slight Reinforcements

35. **Sarangapani G., Reddy B.V. Venkatarama, Jagadish K.S.:** Structural characteristics of bricks, mortars and masonry

36. **Gairns David A, Scrivener; University of Melbourne, Australia:** The effect of masonry unit characteristics on panel lateral capacity

37. **Atkinson R.H., Kingsley G.R., Saeb S., Amadei B., Sture S.; University of Colorado, USA:** A laboratory and in situ study of the shear strength of masonry bed joints

38. **Stöckl Siegfried, Hofmann Peter:** Tests on the shear bond behavior in the bed-joints of masonry

39. **Styliandis Kosmas C.; University of Thessaloniki, Greece:** Cyclic behavior of infilled RC frames

40. **Andreaus Ugo; University of Rome:** A 3-D finite element model for the analysis of masonry structures

41. **Shah Uma Shankar, Institute of Engineering Pulchowk:** M.SC. Thesis (2002)

Appendix A

List of Figures

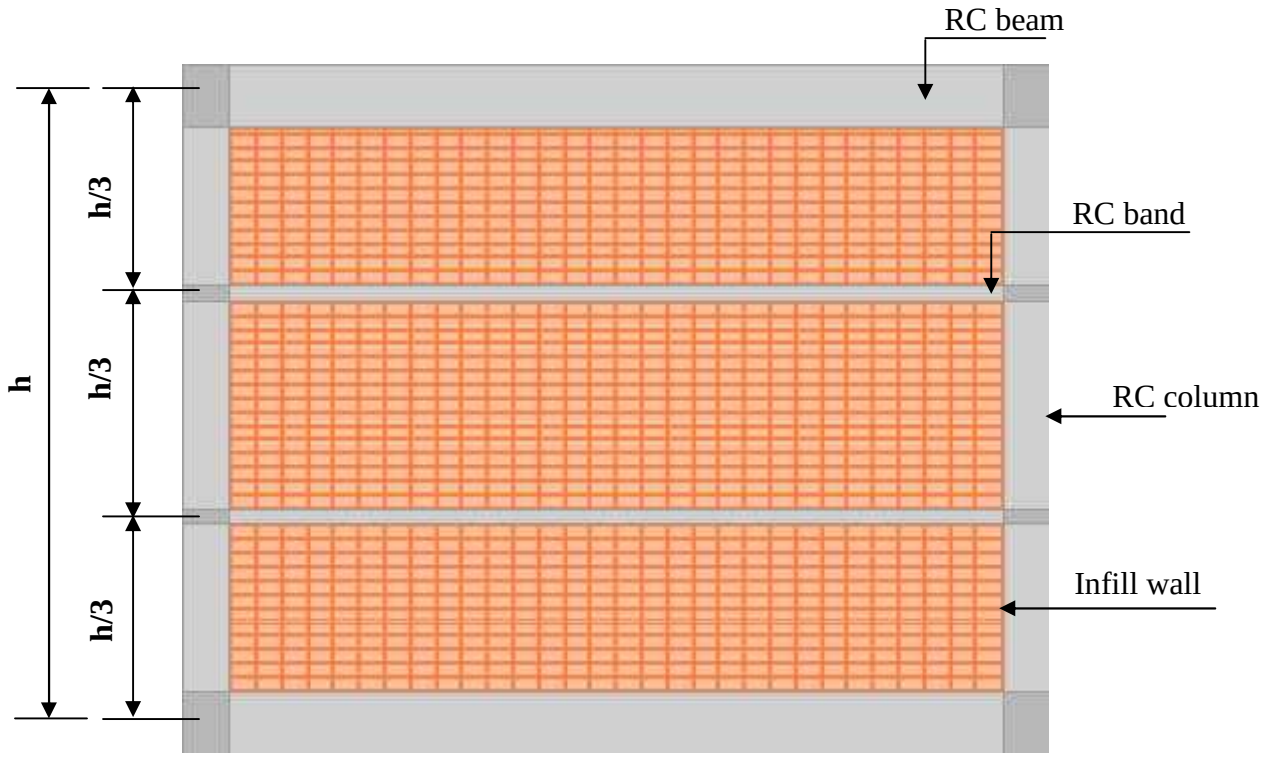

Infill wall with RC bands at one third and two third wall

Fig-A1

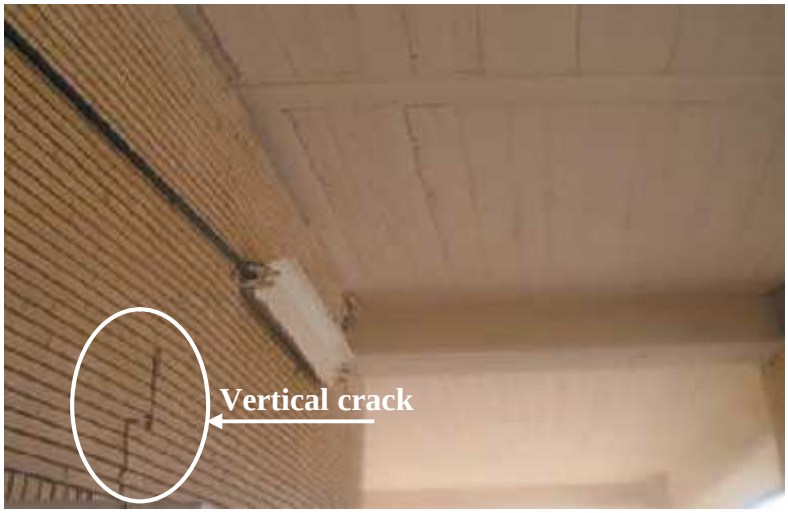

Wall shearing tendency to fail in orthogonal direction (Bam, Iran)

Fig-A2

Damage to Infill wall only in Gölcük

Fig-A3

Construction of bare frame first

Fig-A4

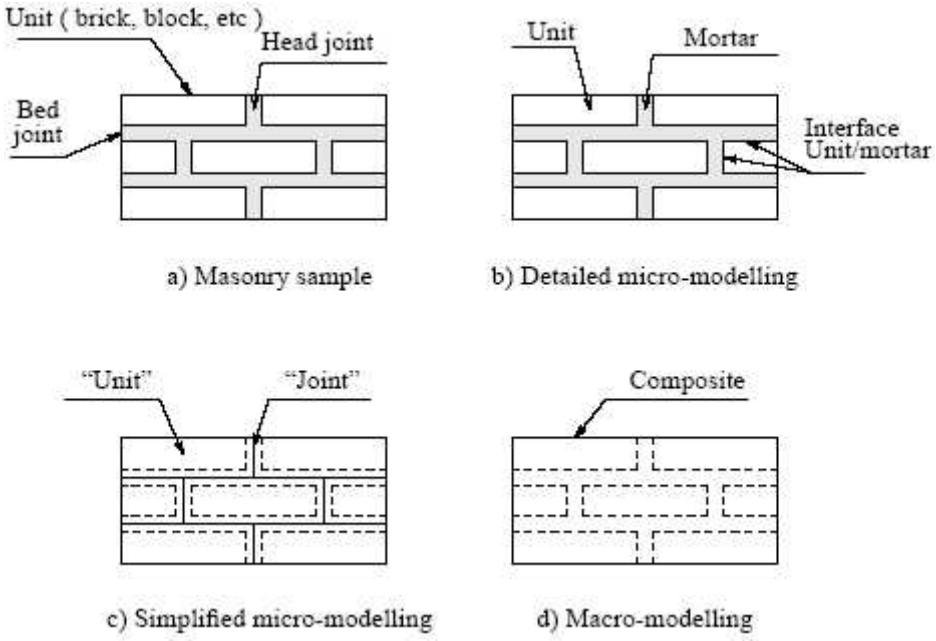

Different modeling techniques of masonry wall adopted in literature

Fig-A5

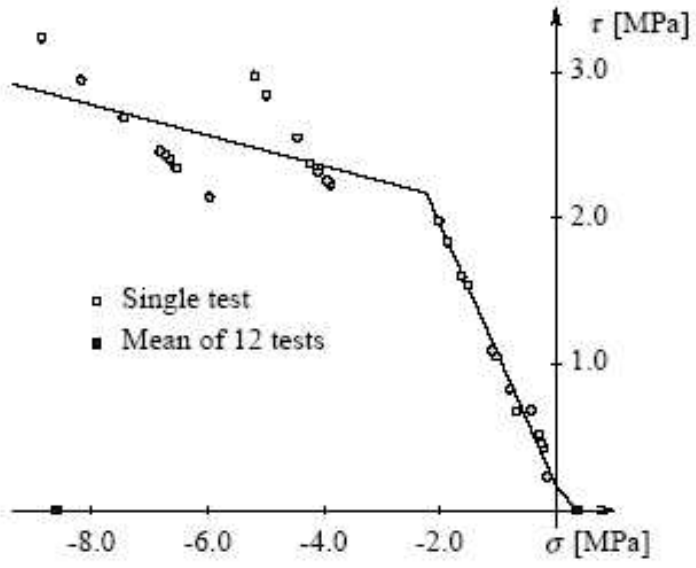

Interface failure envelope (Page 1978)

Fig-A6

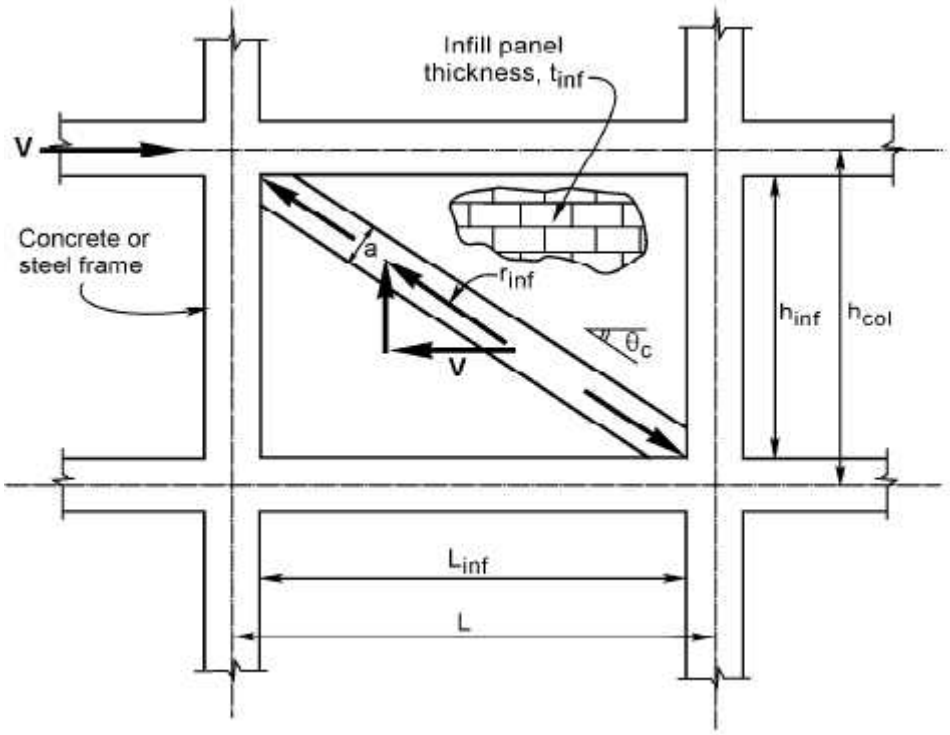

Modeling the infill panel as an equivalent strut (FEMA 306)

Fig-A7

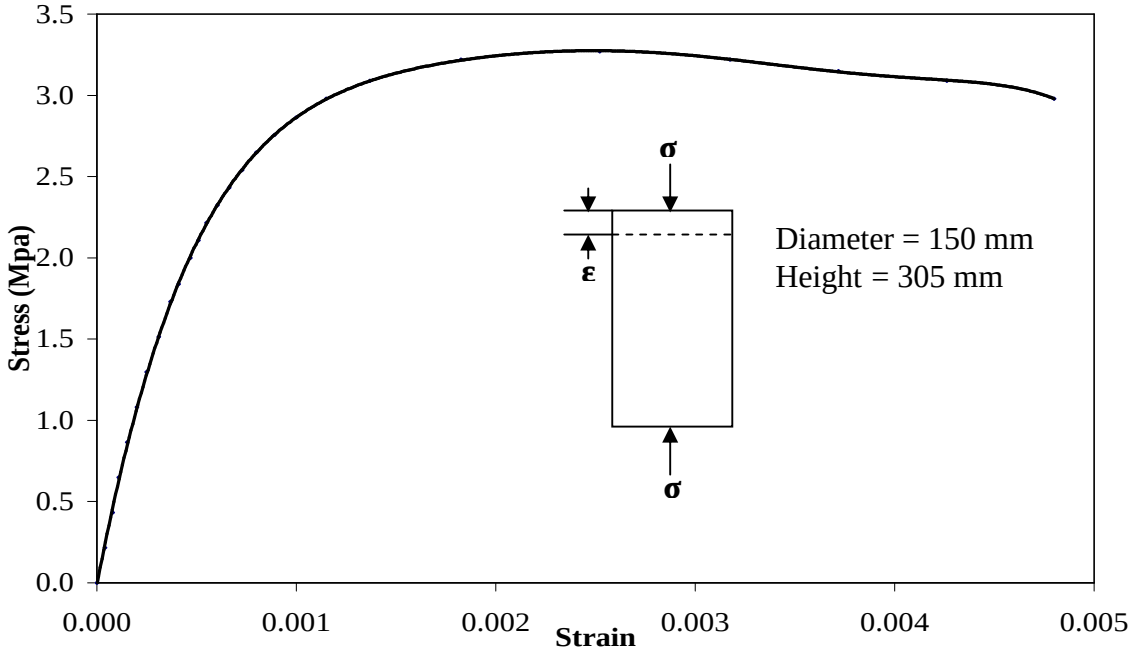

Compressive stress versus longitudinal strain for mortar (1:6)

Fig-A8

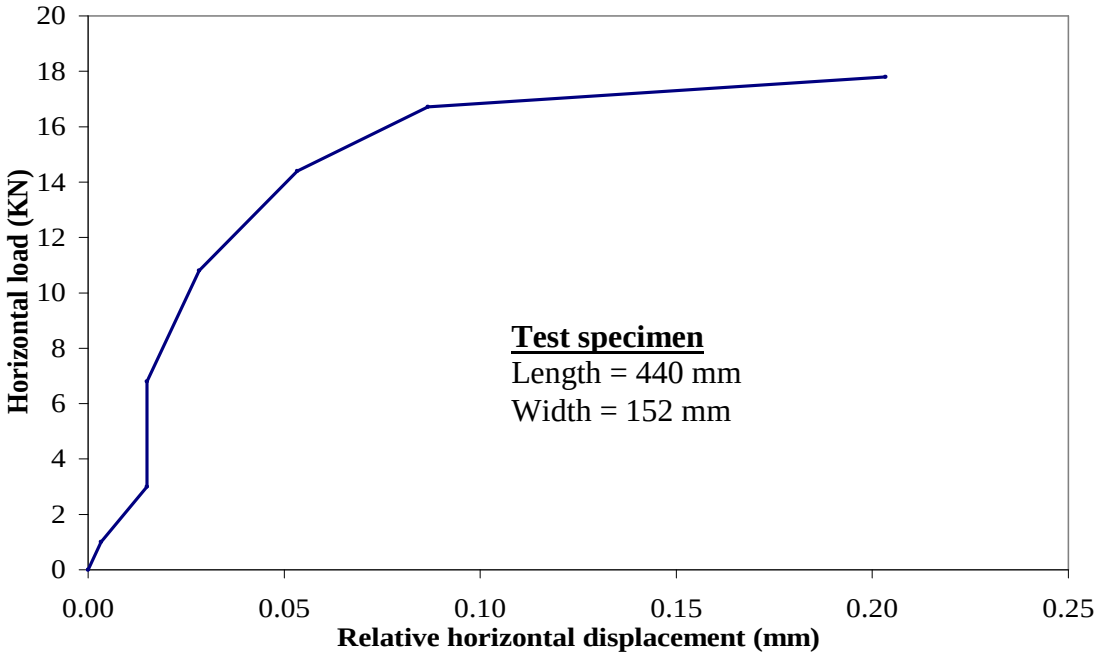

Shear load relative shear displacement response curve

Fig-A9

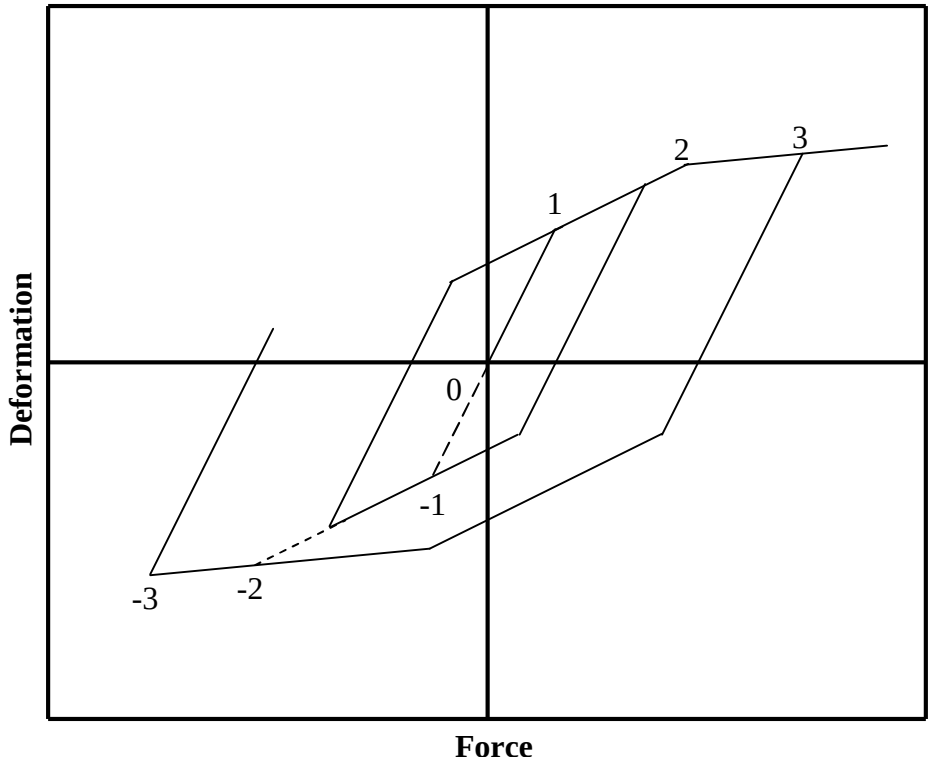

Multi-linear Kinematic Plasticity Property Type for Uniaxial Deformation

Fig- A10

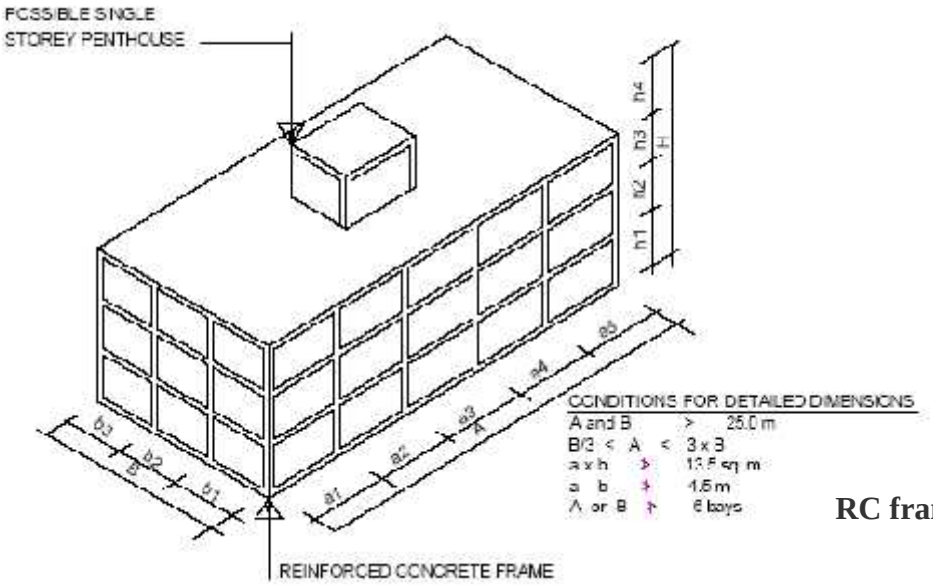

RC frame (NBC 201:1994)

Fig-A11

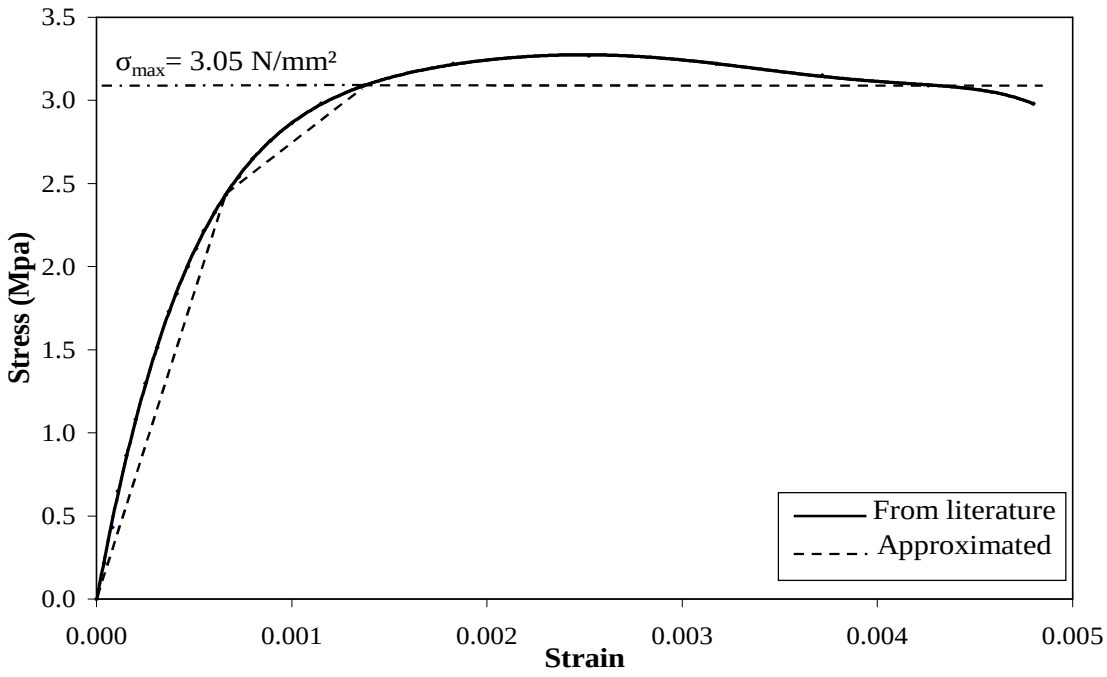

Compressive stress versus longitudinal strain for mortar (1:6)

Fig-A12

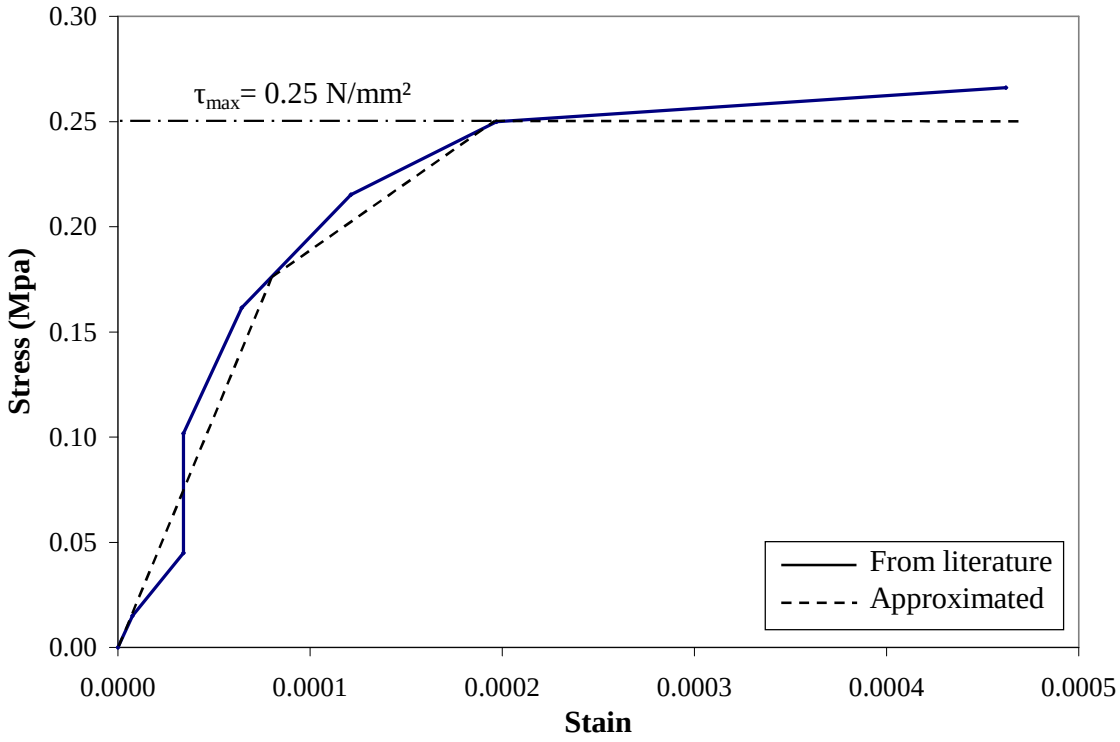

Shear stress-strain curve for mortar (1:6)

Fig-A13

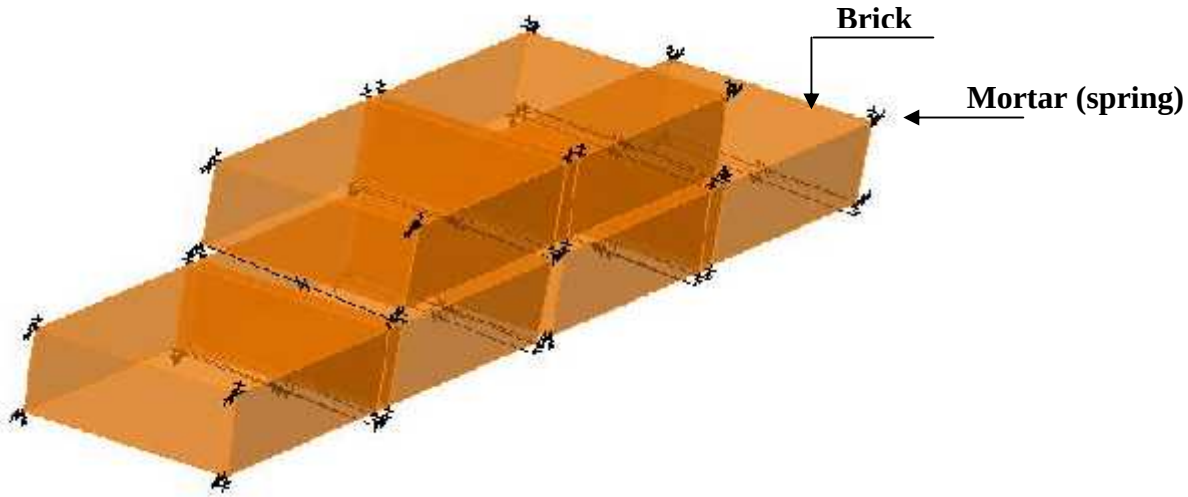

Modeling detail of brick and mortar

Fig-A14

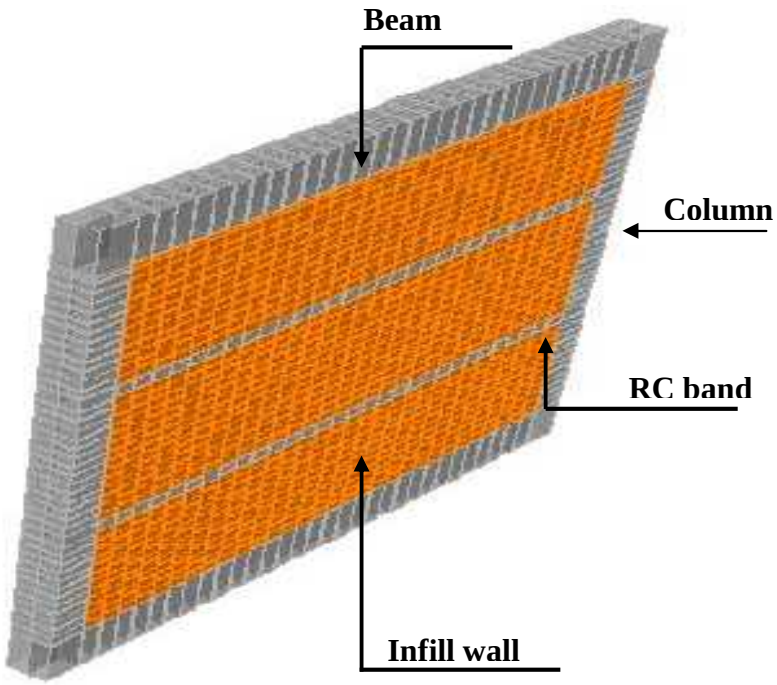

Infill wall model with band

Fig-A15

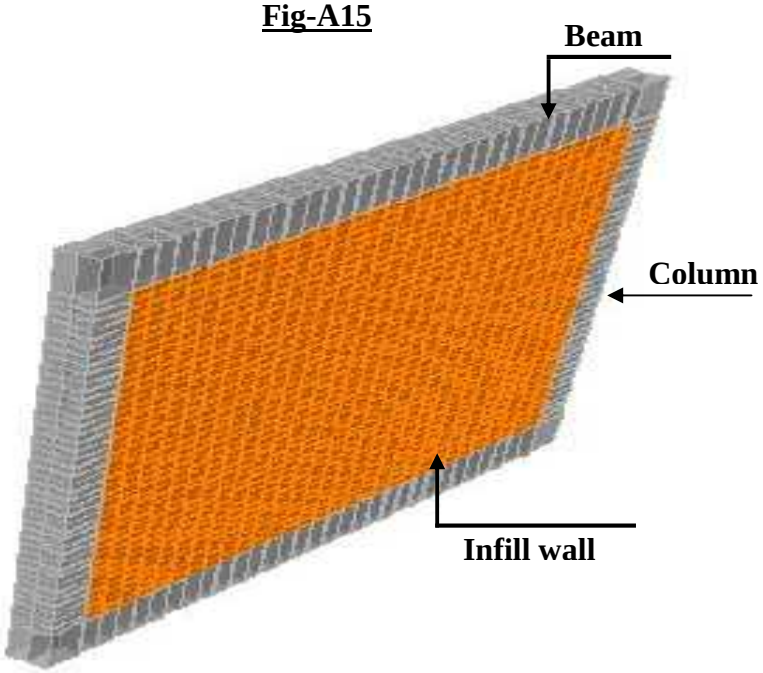

Infill wall model without band

Fig-A16

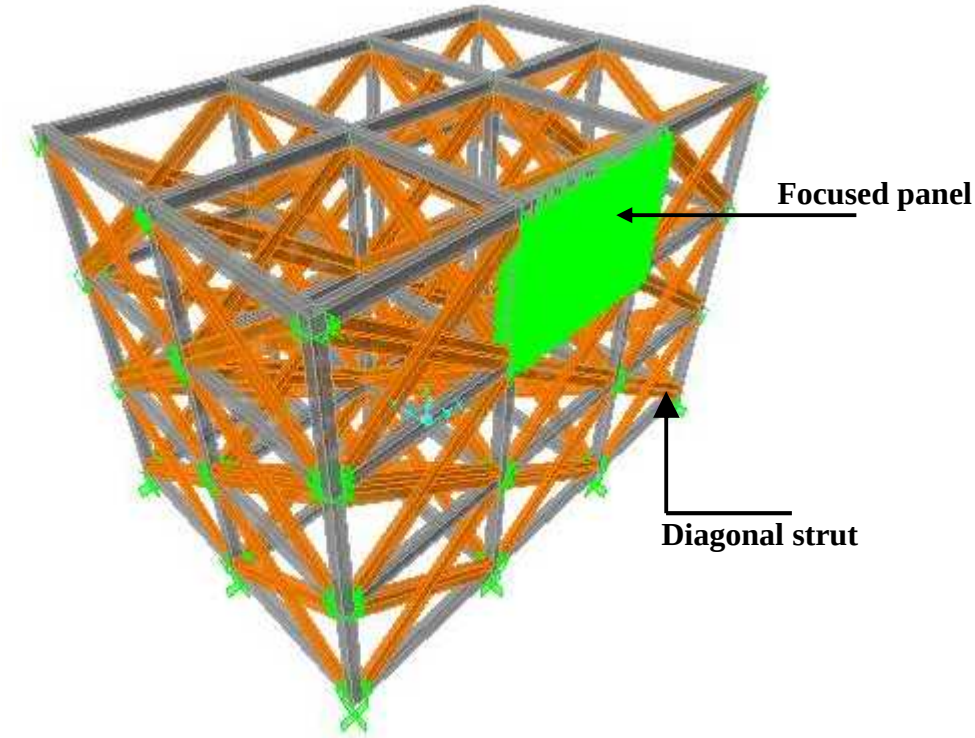

Detail 3-D modeling

Fig-A17

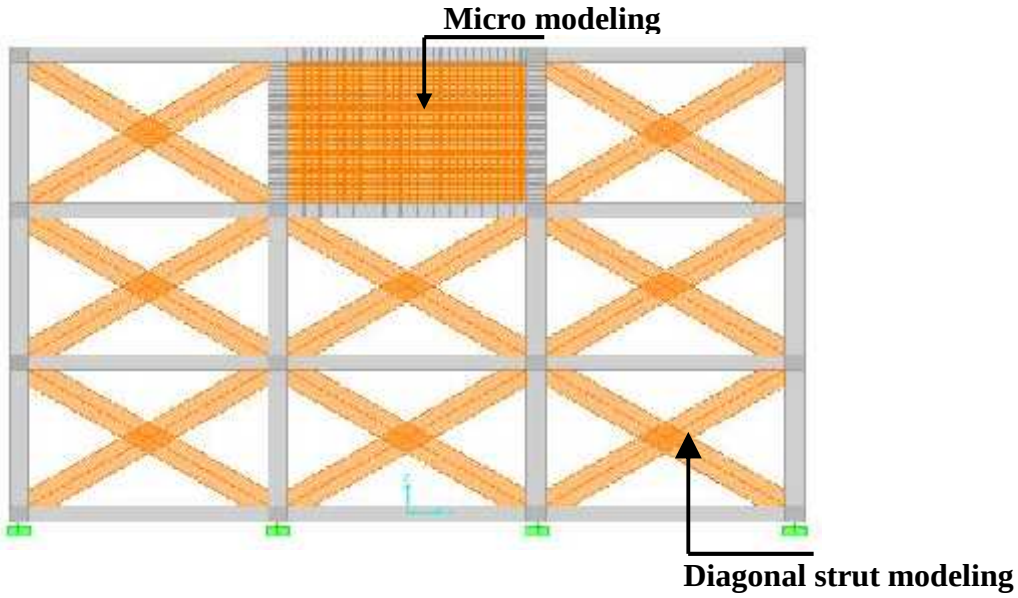

Elevation of model showing micro and equivalent strut modeling

Fig-A18

Appendix B

Output Charts and Graphs

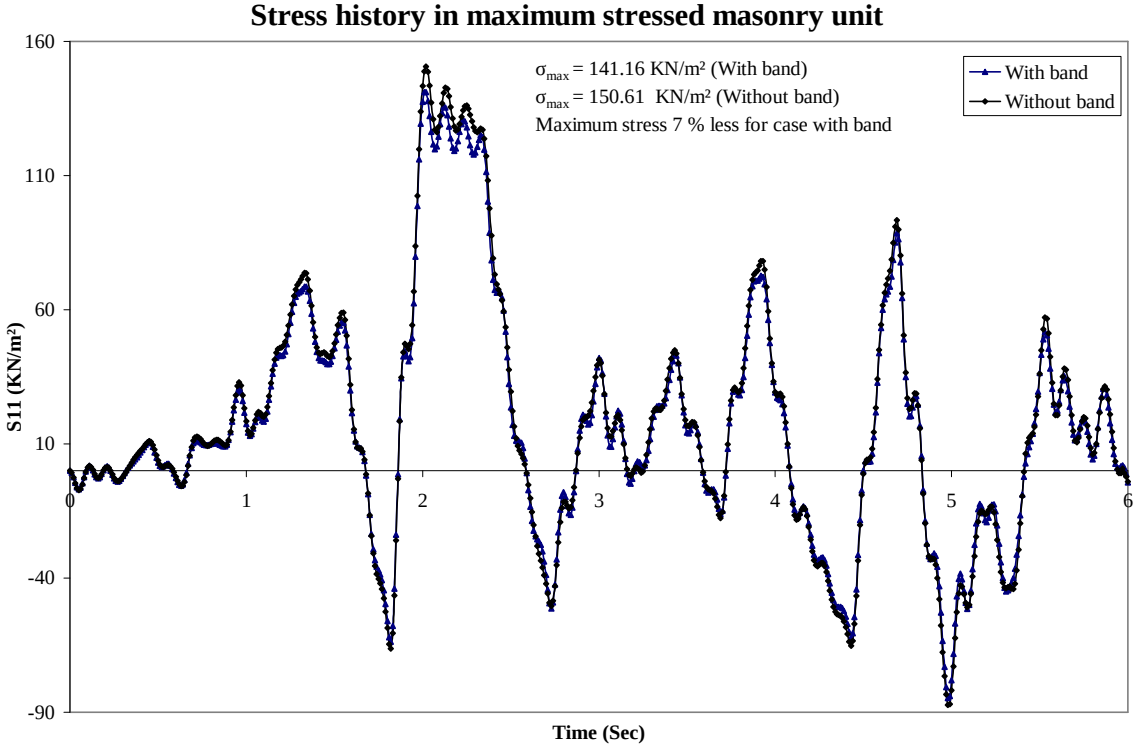
Stress history in maximum stressed masonry unit
σmax = 141.16 KN/m² (With band)
σmax = 150.61 KN/m² (Without band)
Maximum stress 7 % less for case with band
With band
Without band
S11 (KN/m²)
Time (Sec)

Fig-B1

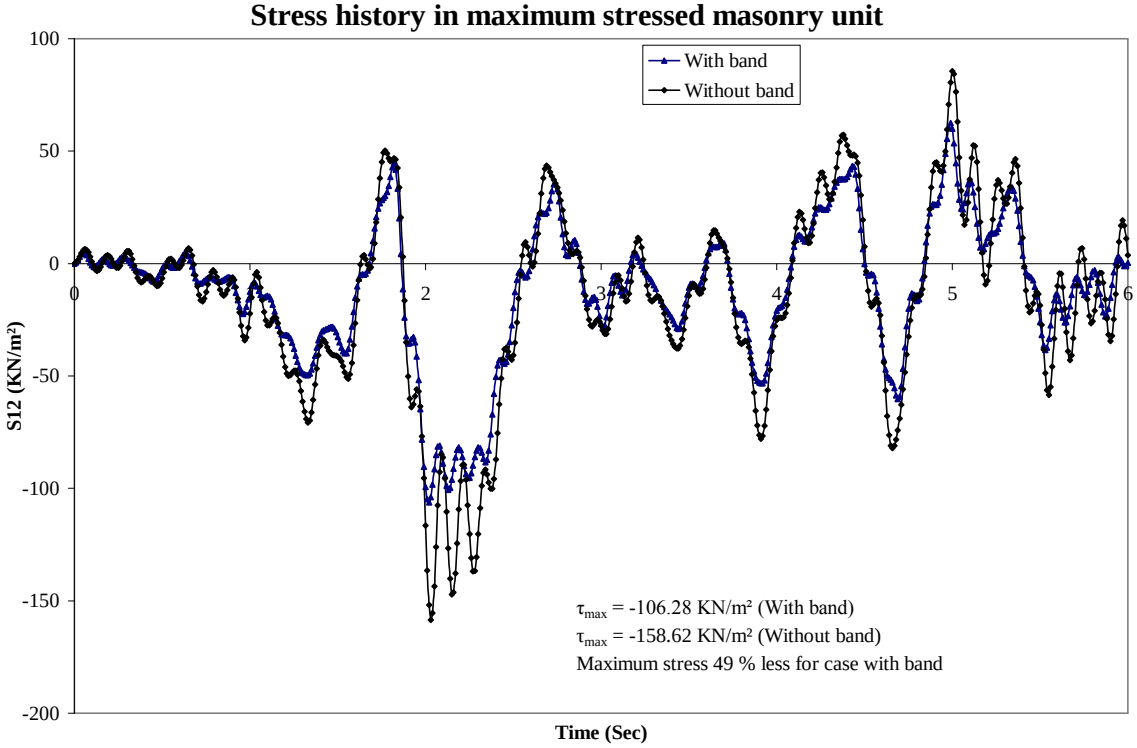
Stress history in maximum stressed masonry unit
With band
Without band
τmax = -106.28 KN/m² (With band)
τmax = -158.62 KN/m² (Without band)
Maximum stress 49 % less for case with band
S12 (KN/m²)
Time (Sec)

Fig –B2

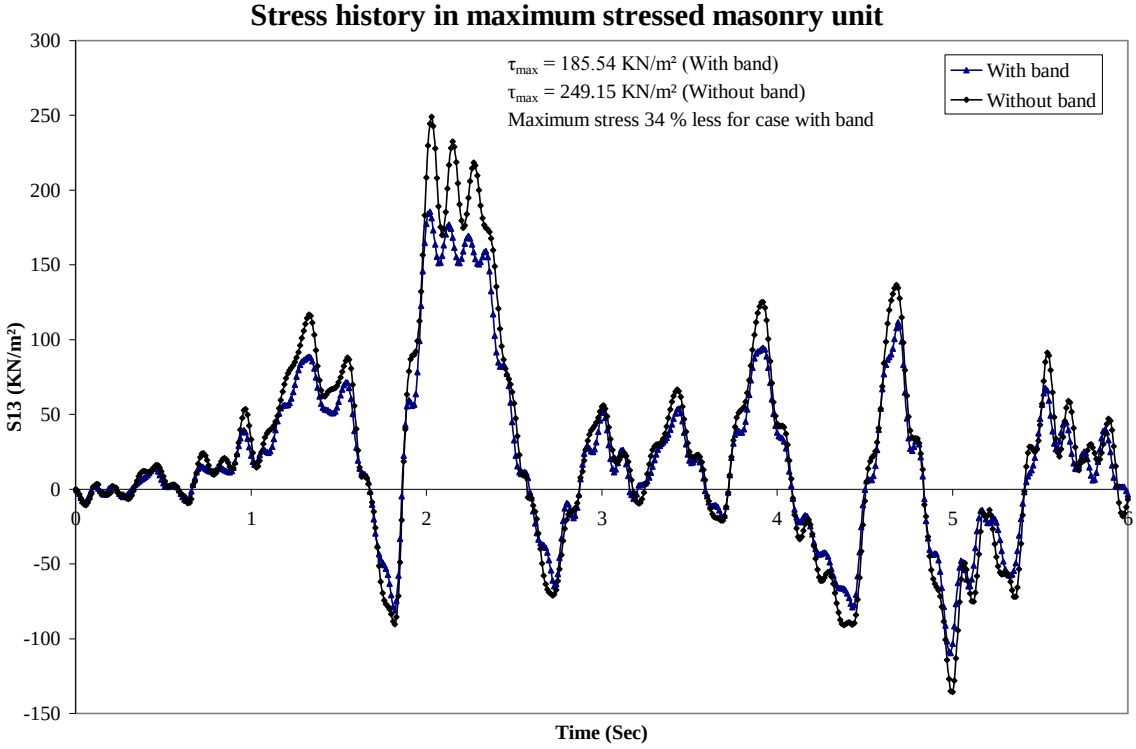
Stress history in maximum stressed masonry unit
τmax = 185.54 KN/m² (With band)
τmax = 249.15 KN/m² (Without band)
Maximum stress 34 % less for case with band
With band
Without band
S13 (KN/m²)
Time (Sec)

Fig-B3

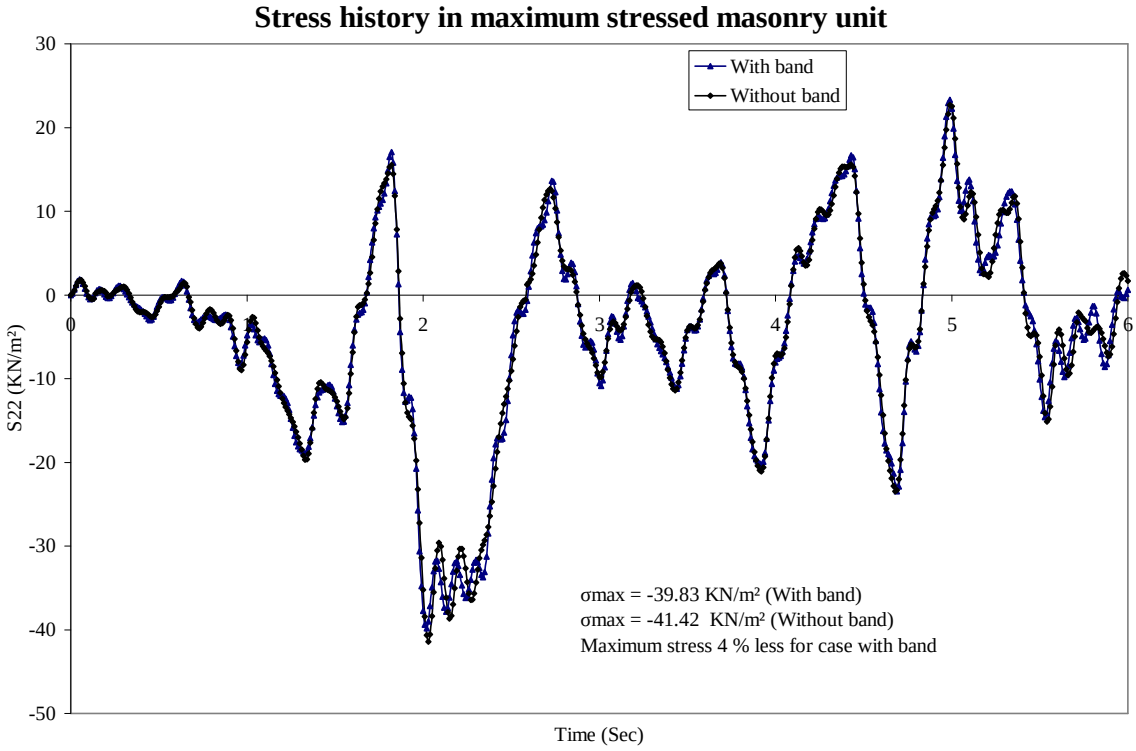
Stress history in maximum stressed masonry unit
With band
Without band
σmax = -39.83 KN/m² (With band)
σmax = -41.42 KN/m² (Without band)
Maximum stress 4 % less for case with band
S22 (KN/m²)
Time (Sec)

Fig-B4

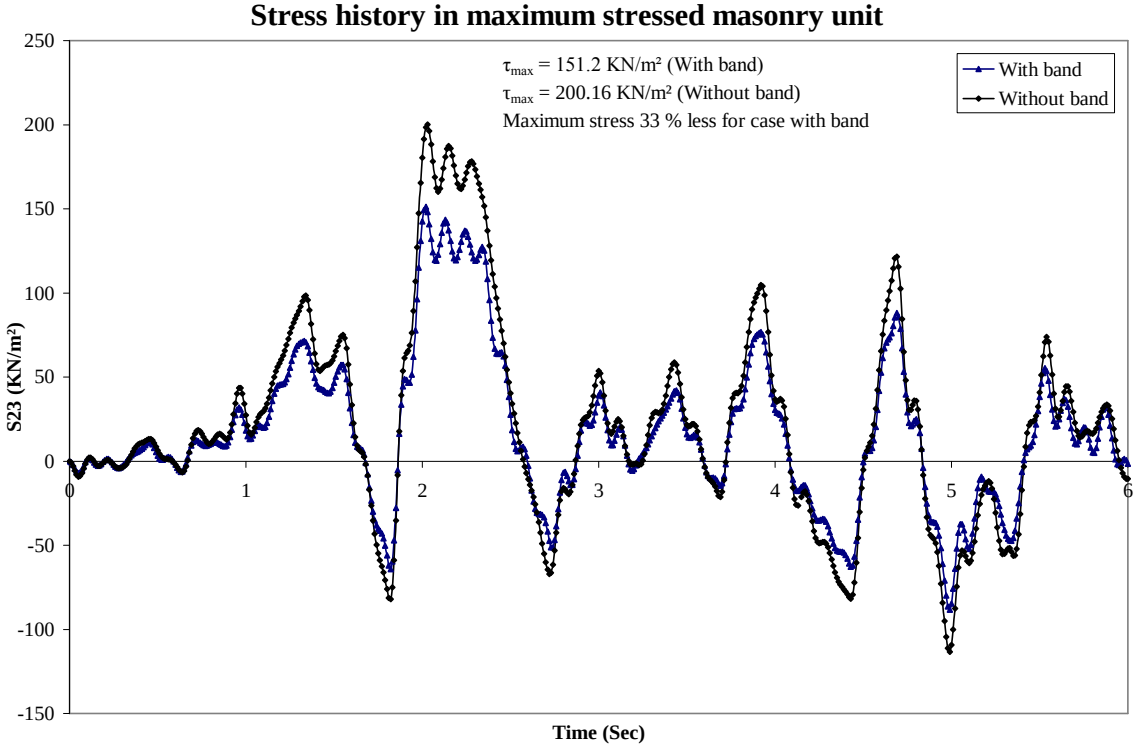
Stress history in maximum stressed masonry unit
τmax = 151.2 KN/m² (With band)
τmax = 200.16 KN/m² (Without band)
Maximum stress 33 % less for case with band
With band
Without band
S23 (KN/m²)
Time (Sec)

Fig-B5

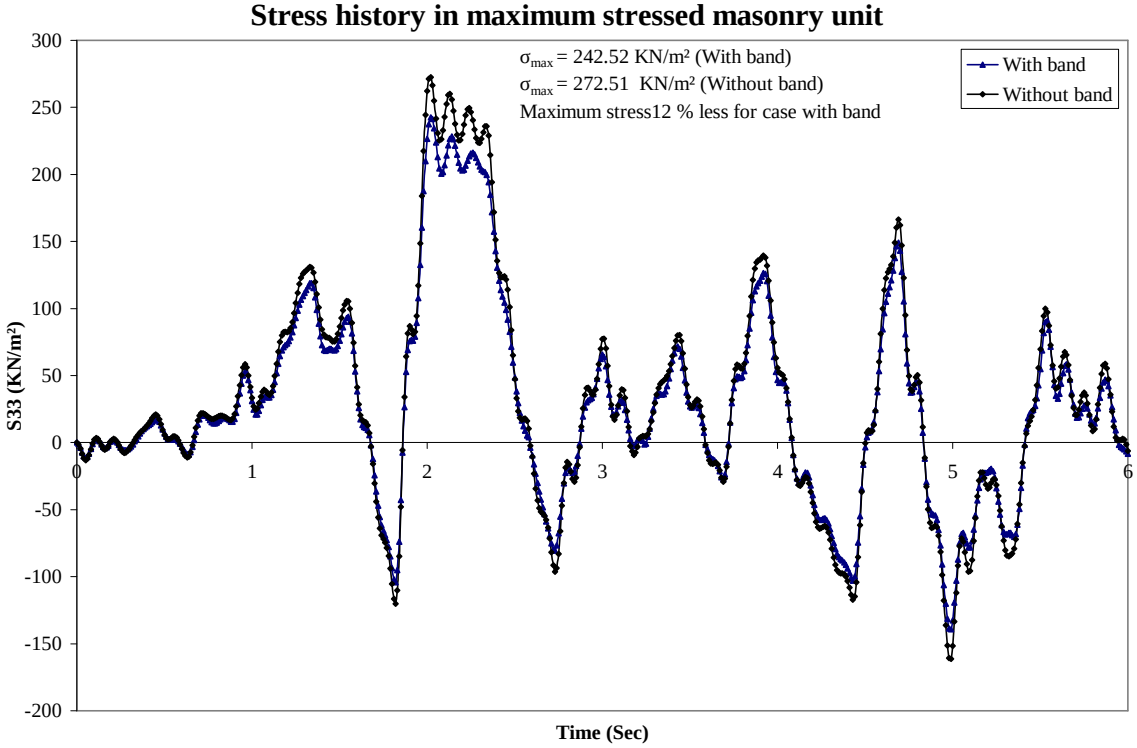
Stress history in maximum stressed masonry unit
σmax = 242.52 KN/m² (With band)
σmax = 272.51 KN/m² (Without band)
Maximum stress12 % less for case with band
With band
Without band
S33 (KN/m²)
Time (Sec)

Fig-B6

Displacement history of maximum displaced point of building (X-direction)

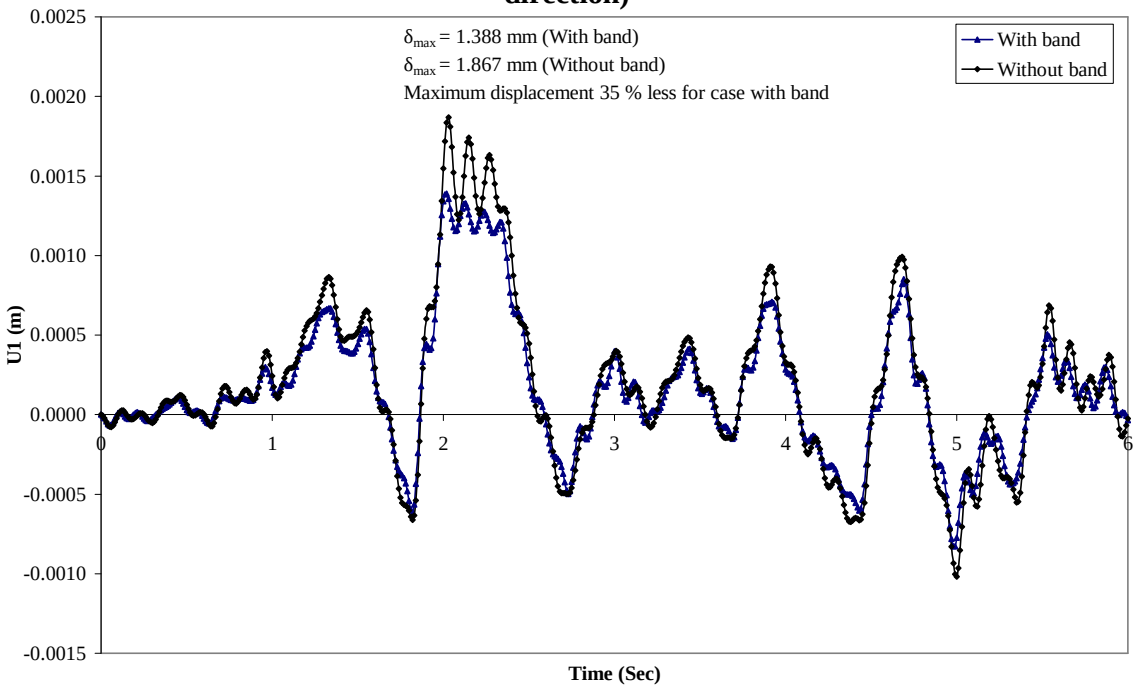

Fig-B7

Displacement history of maximum displaced point of building (Y-direction)

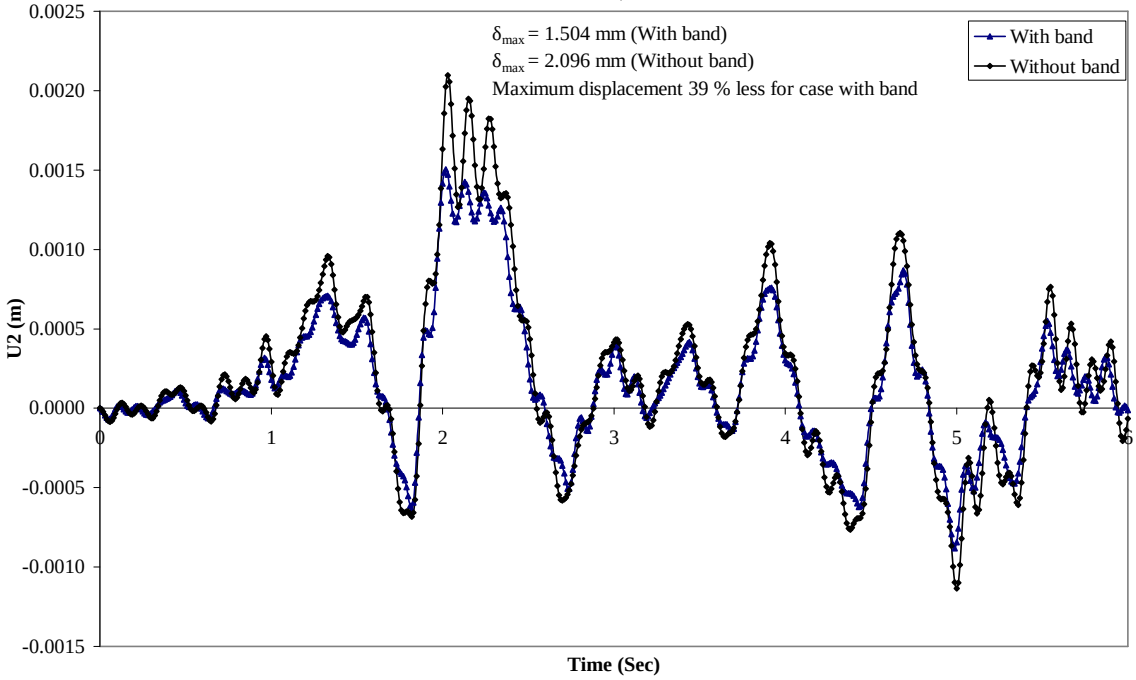

Fig-B8

Displacement history of maximum displaced masonry unit (X-Direction)

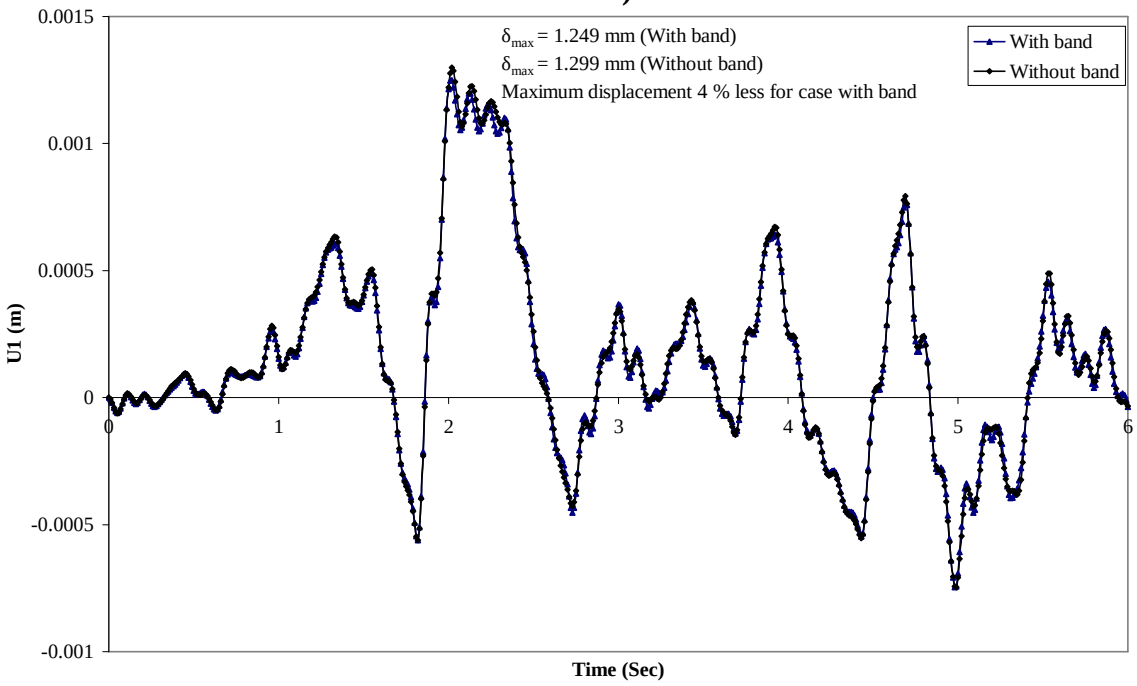

Fig-B9

Displacement history of maximum displaced masonry unit (Y-Direction)

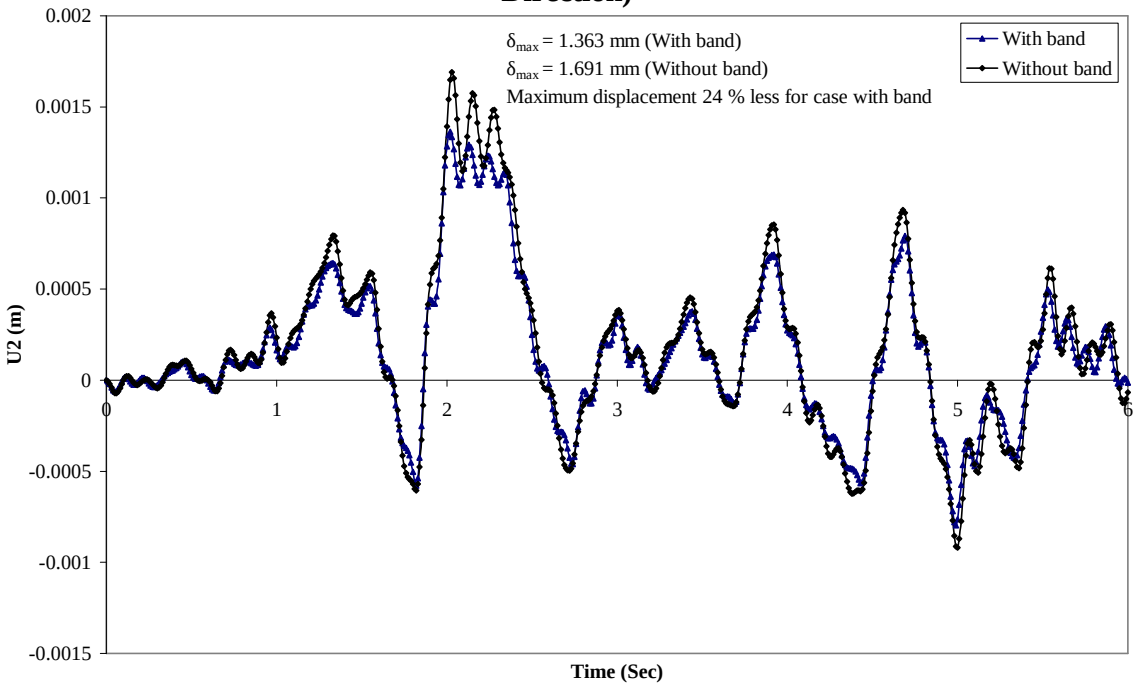

Fig-B10

In-plane displacement of brick with height at left end of wall (X-Direction)

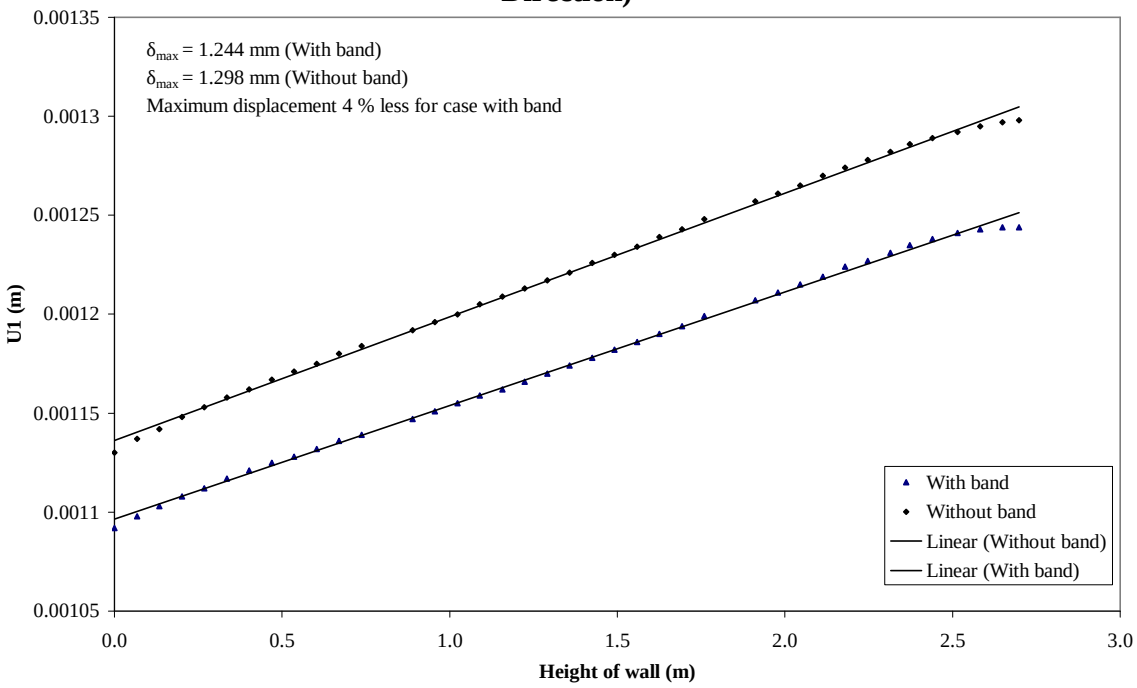

Fig-B11

In-plane displacement of brick with height at mid of wall (X-Direction)

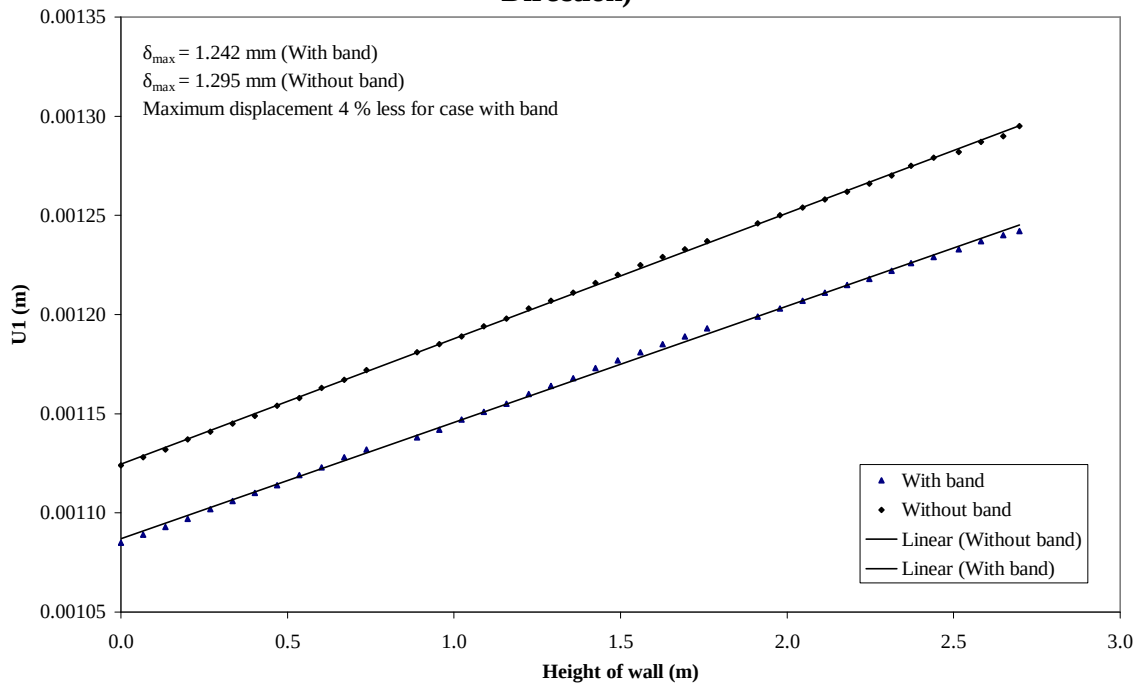

Fig-B12

In-plane displacement of brick with height at right end of wall (X-Direction)

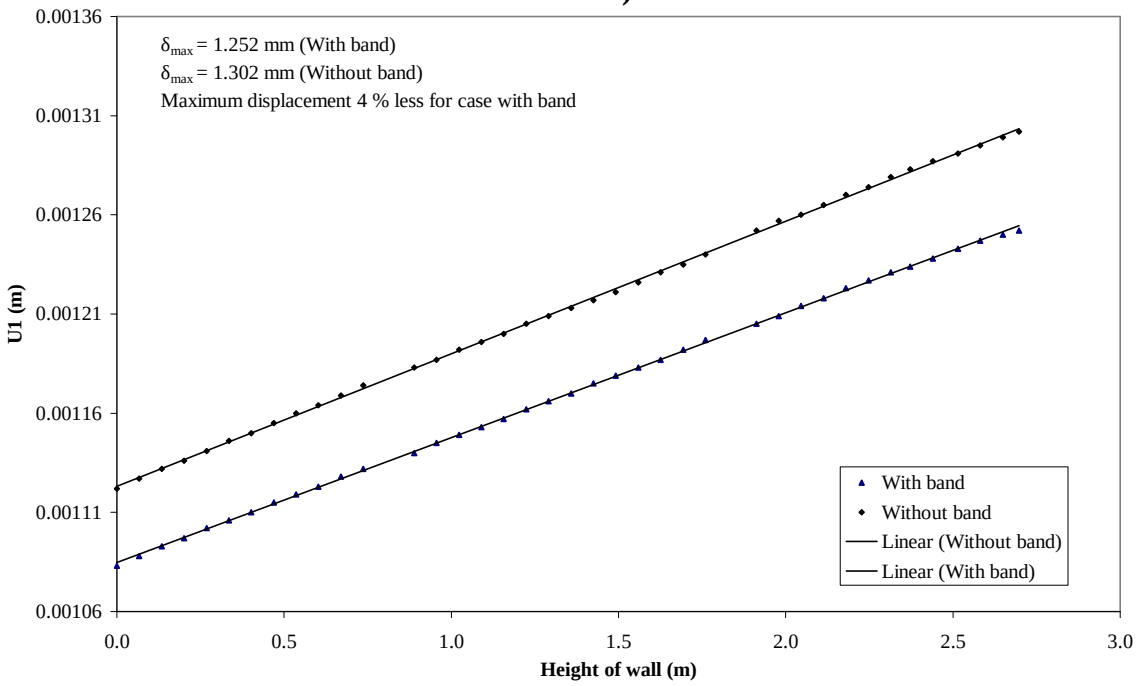

Fig-B13

Out-of-plane displacement of brick with height at left end of wall (Y-Direction)

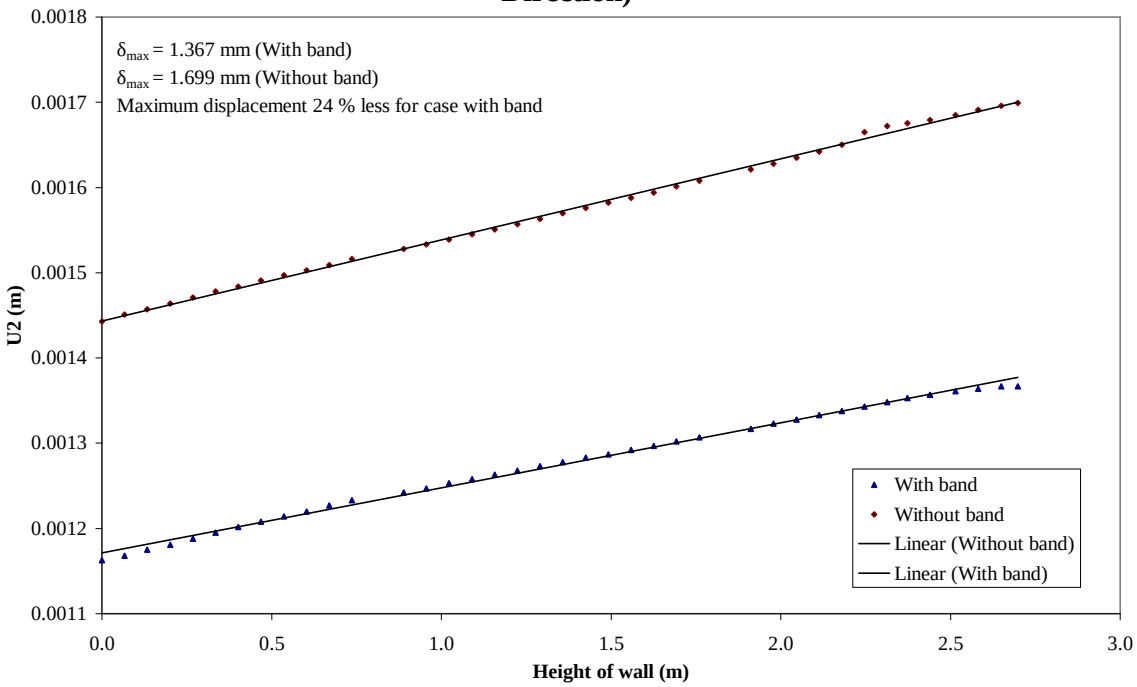

Fig-B14

Out-of-plane displacement of brick with height at mid of wall (Y-Direction)

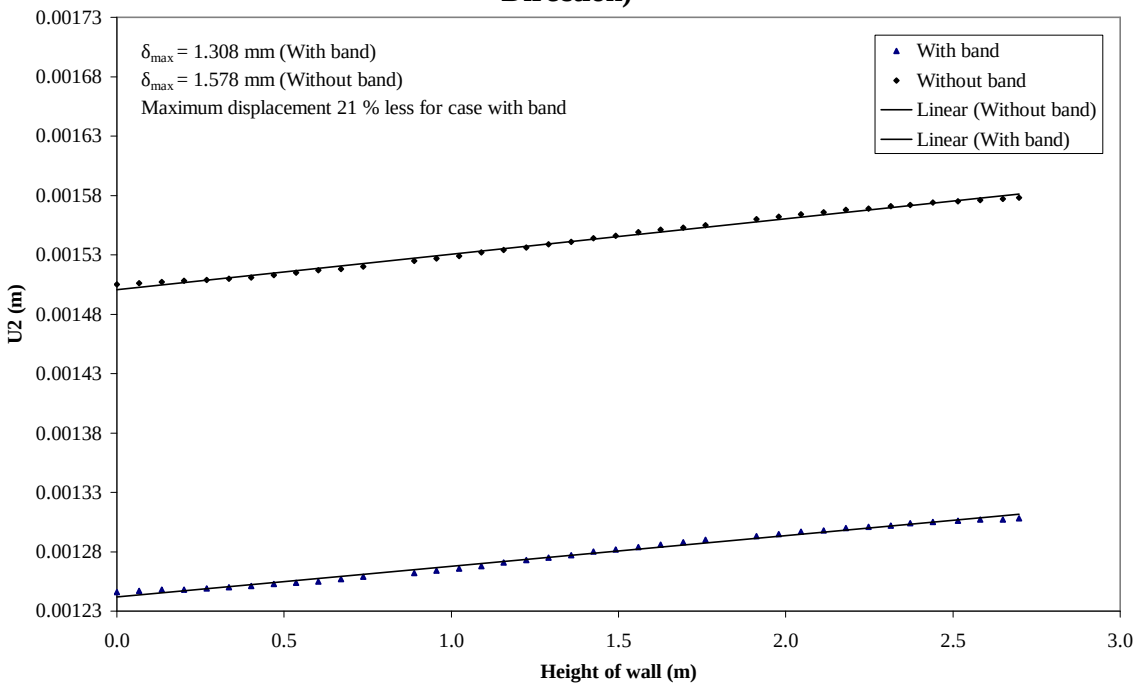

Fig-B15

Out-of-plane displacement of brick with height at right end of wall (Y-Direction)

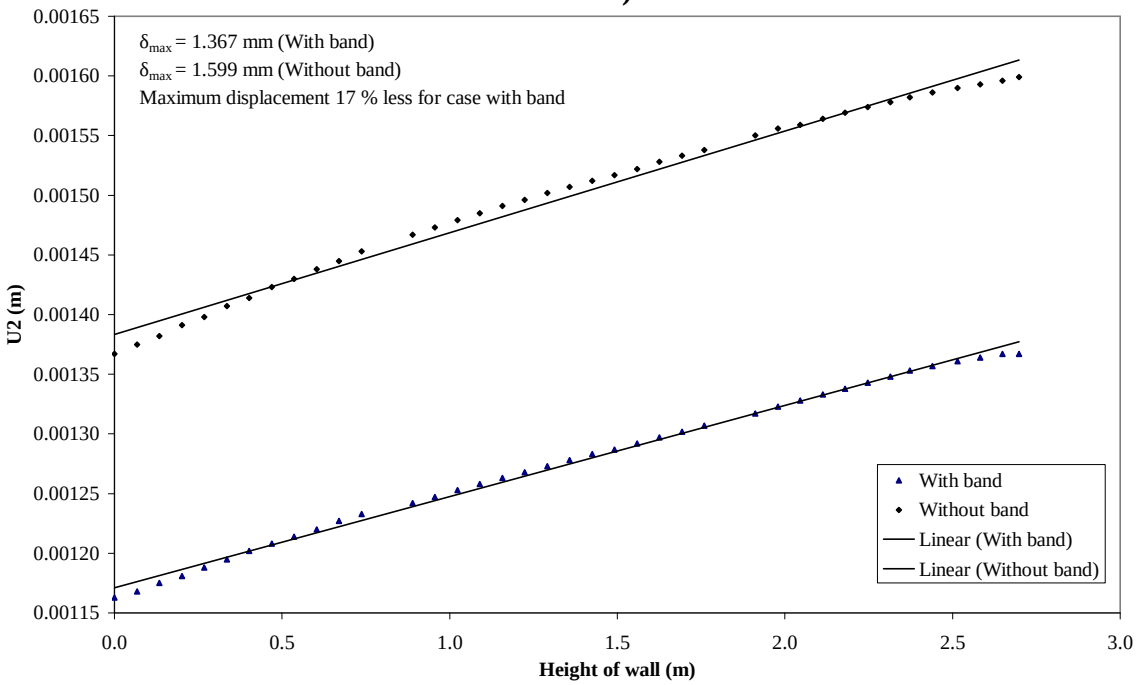

Fig-B16

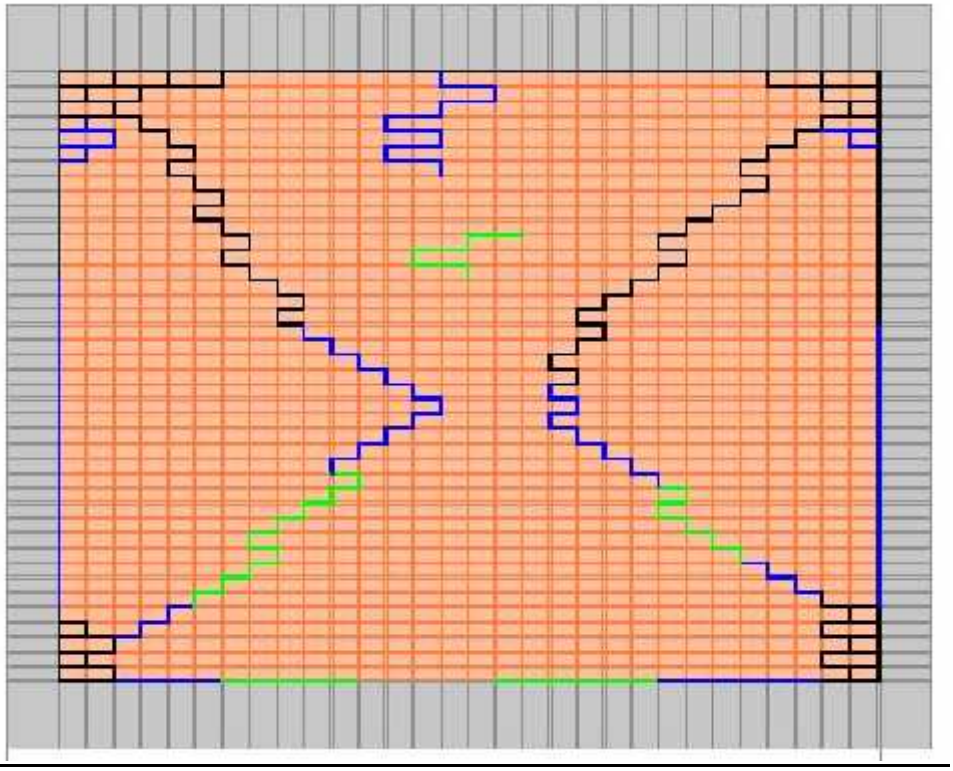

Fig-B17

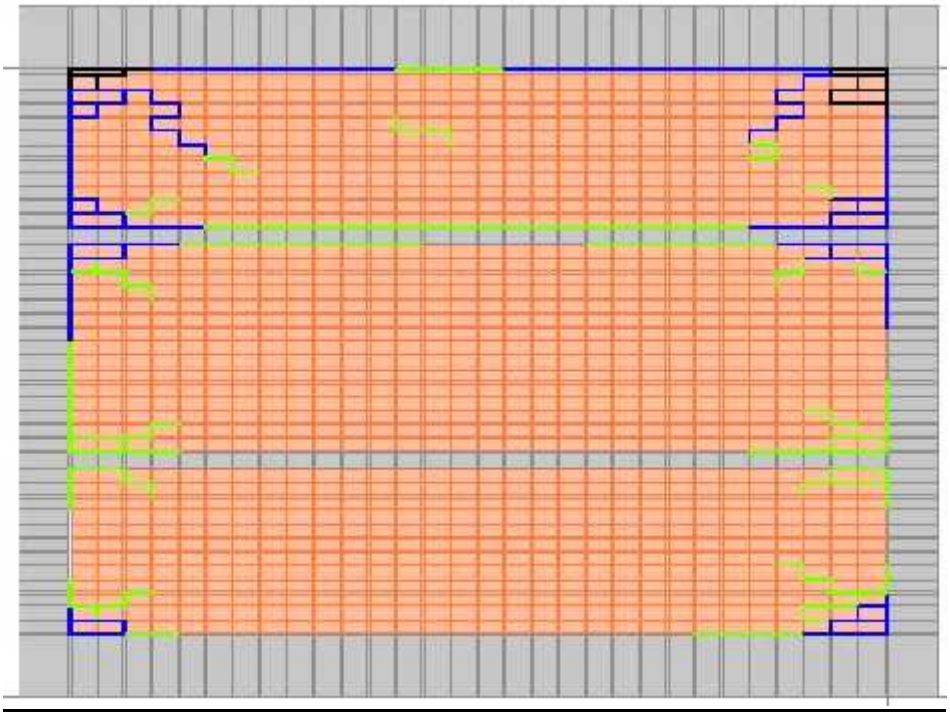

Fig-B18

Stress ≥ 100 % of failure stress
80≤Stress<100 % of failure stress
60≤Stress<80 % of failure stress

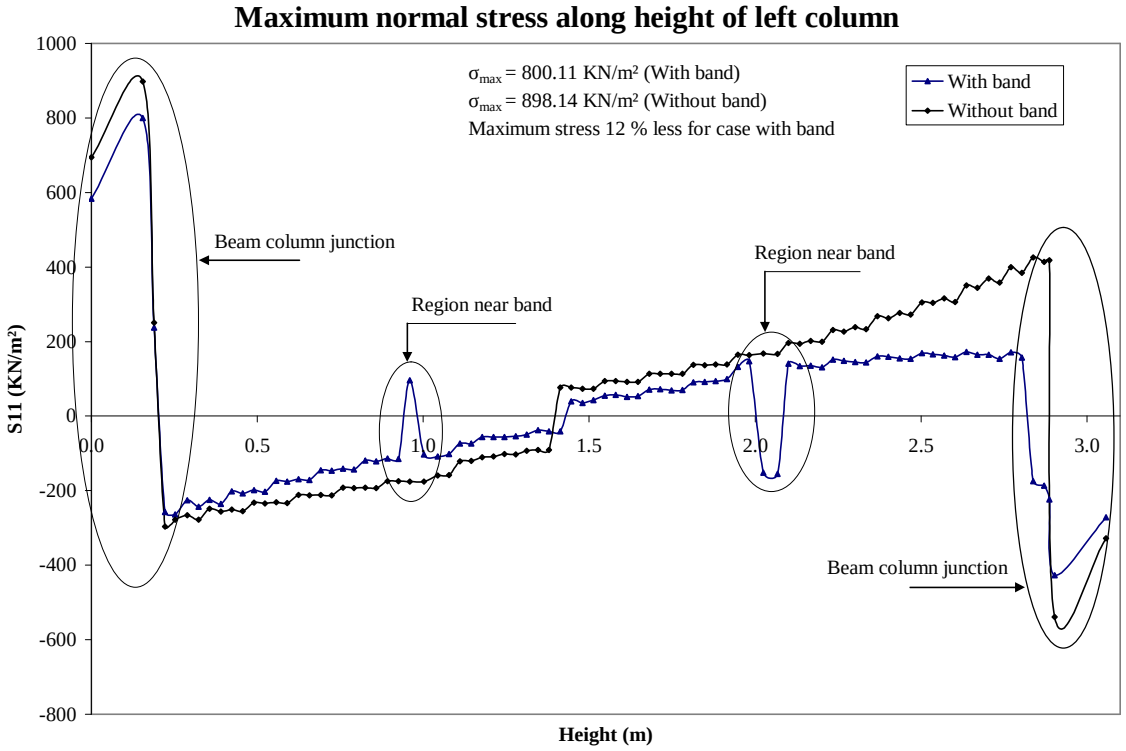

Fig-B19

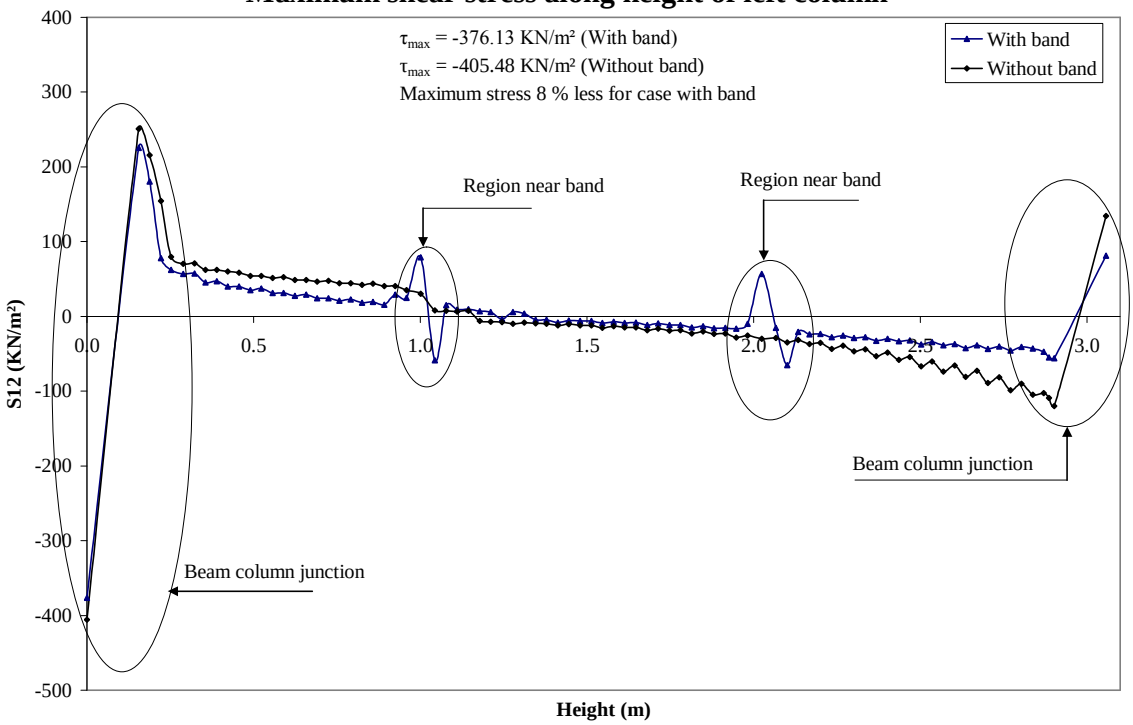

Fig-B20

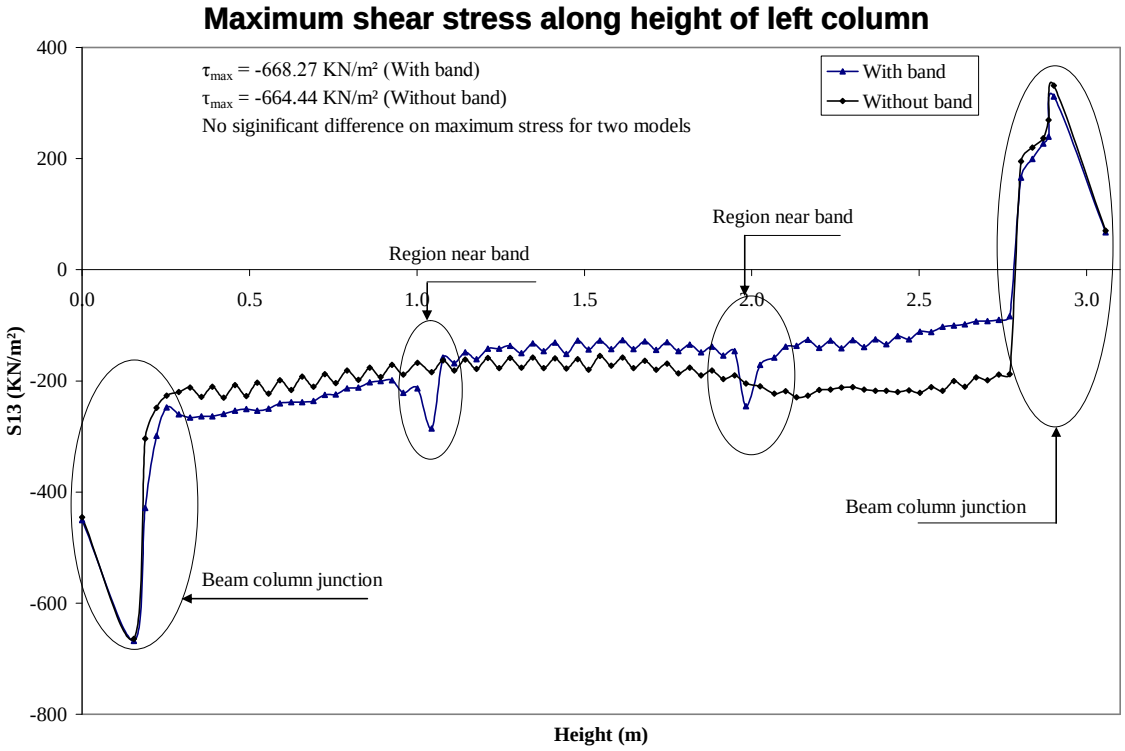

Fig-B21

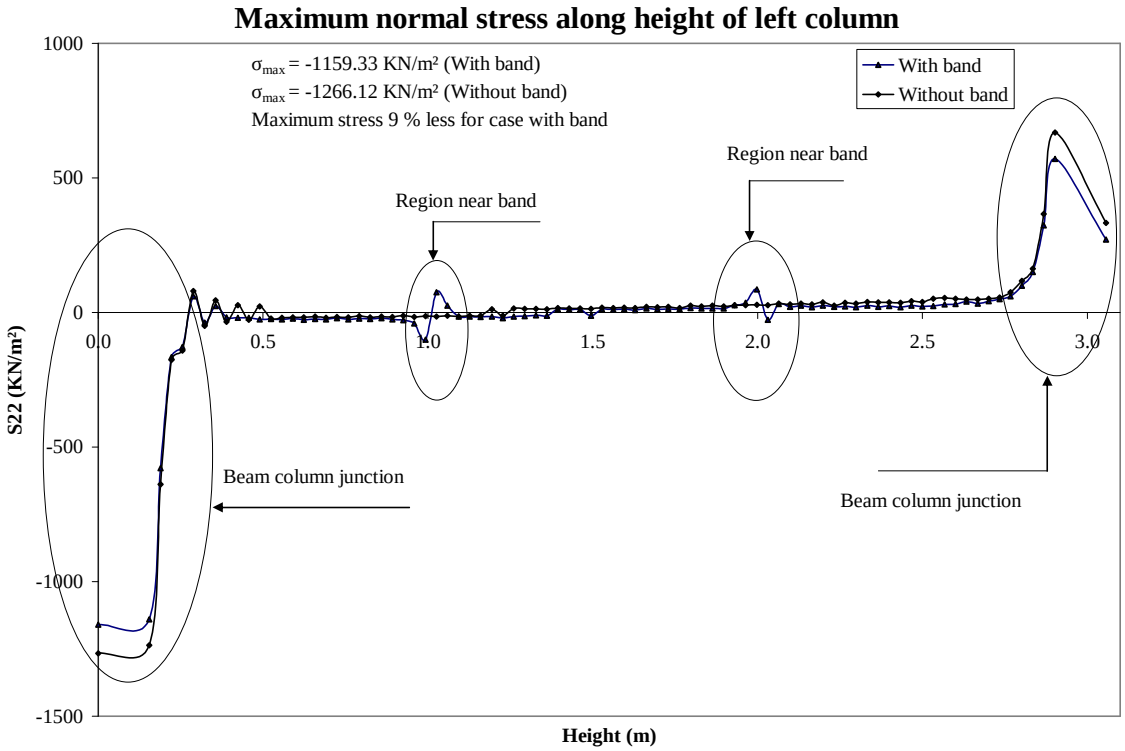

Fig-B22

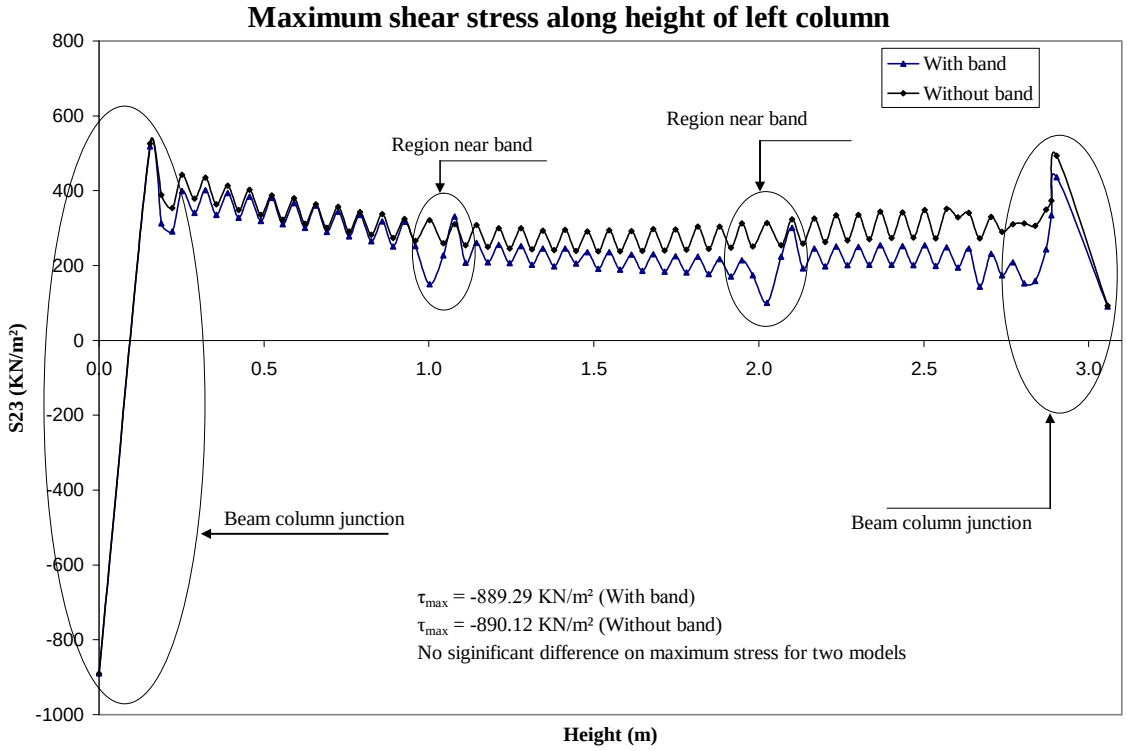

Fig-B23

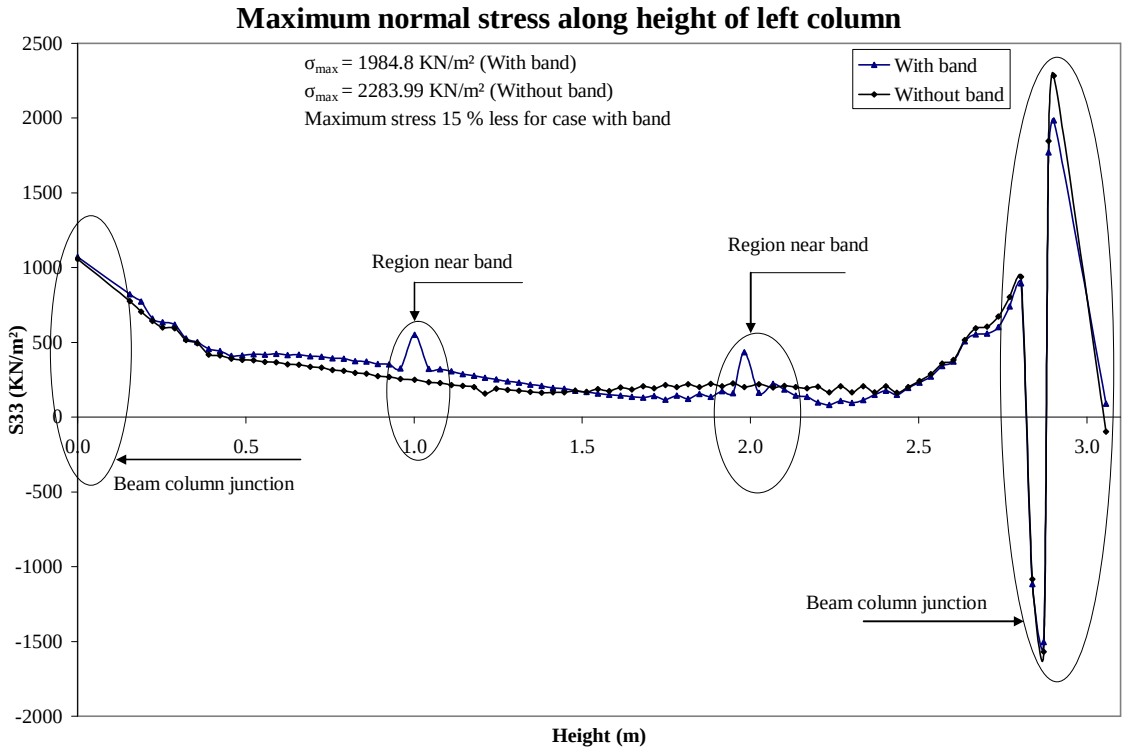

Fig-B24

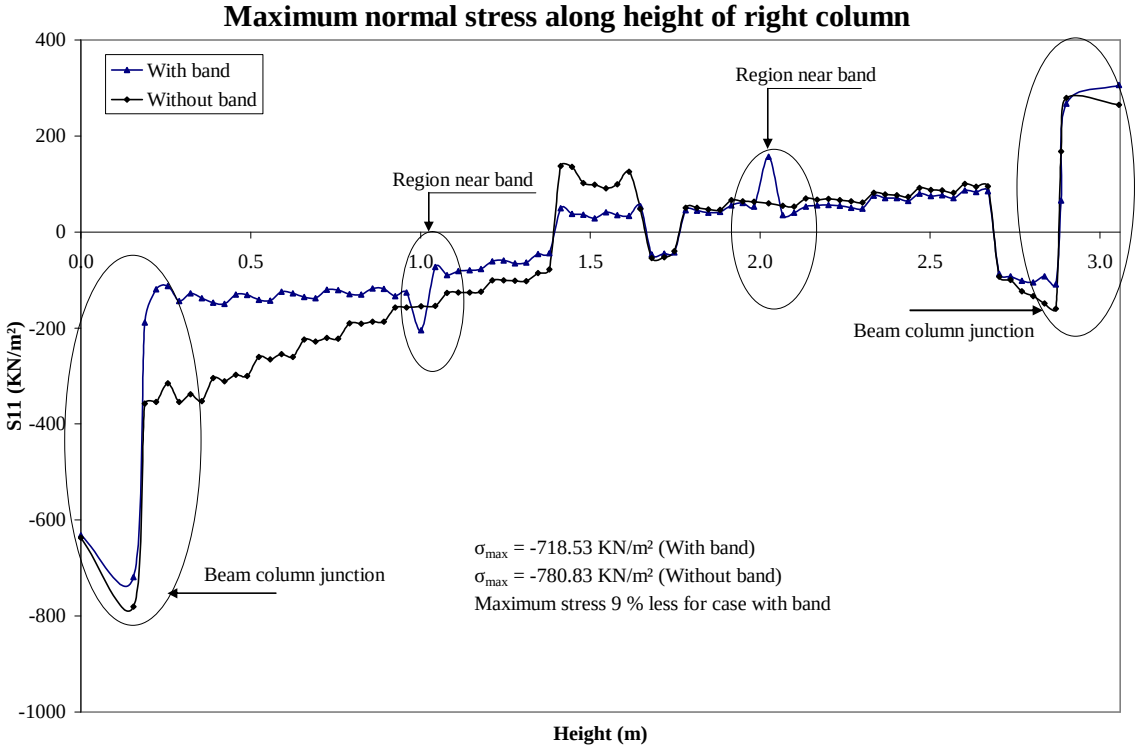

Fig-B25

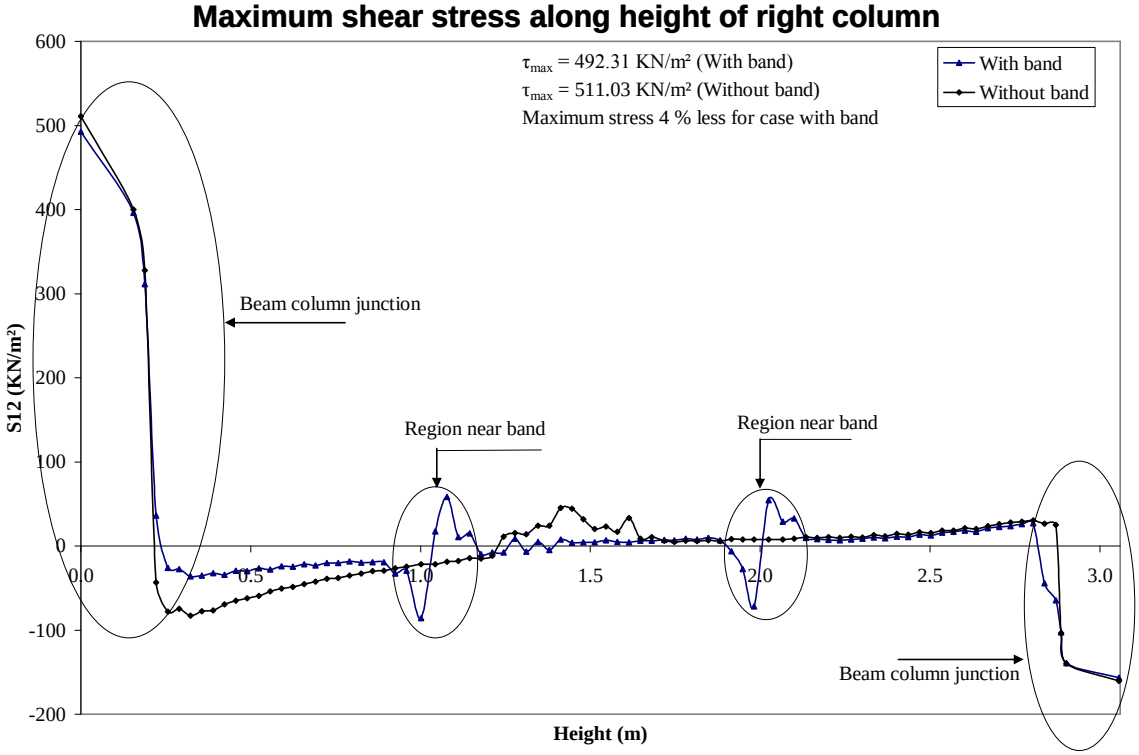

Fig-B26

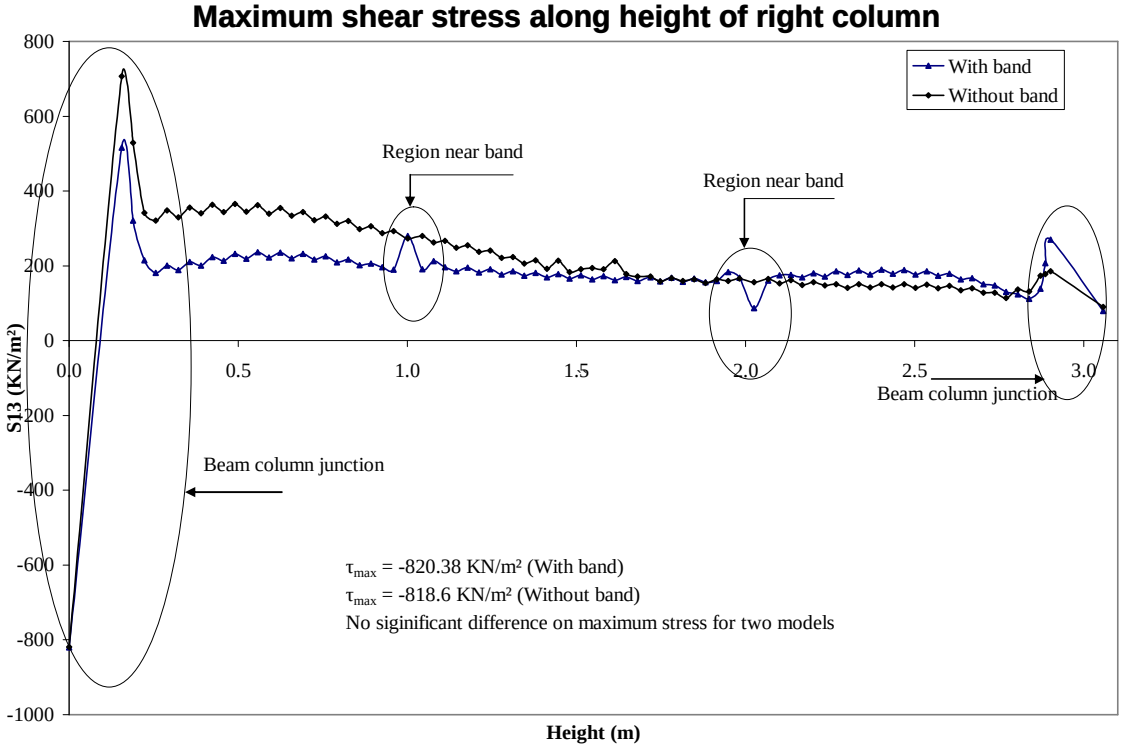

Fig-B27

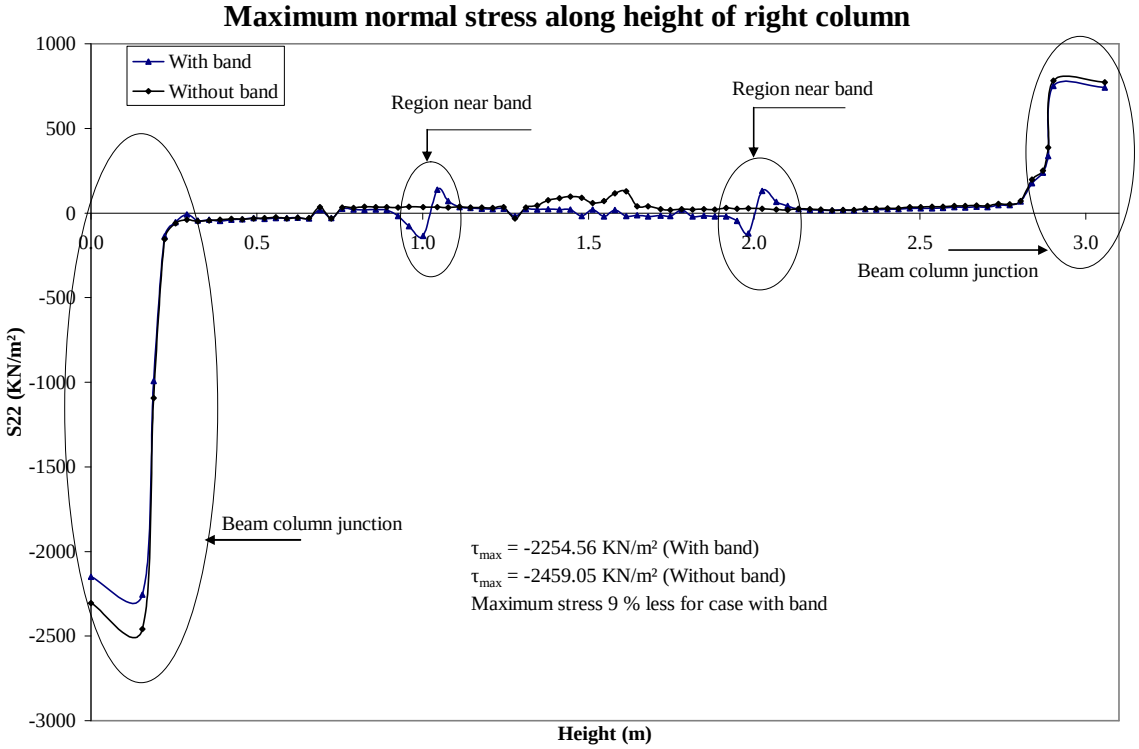

Fig-B28

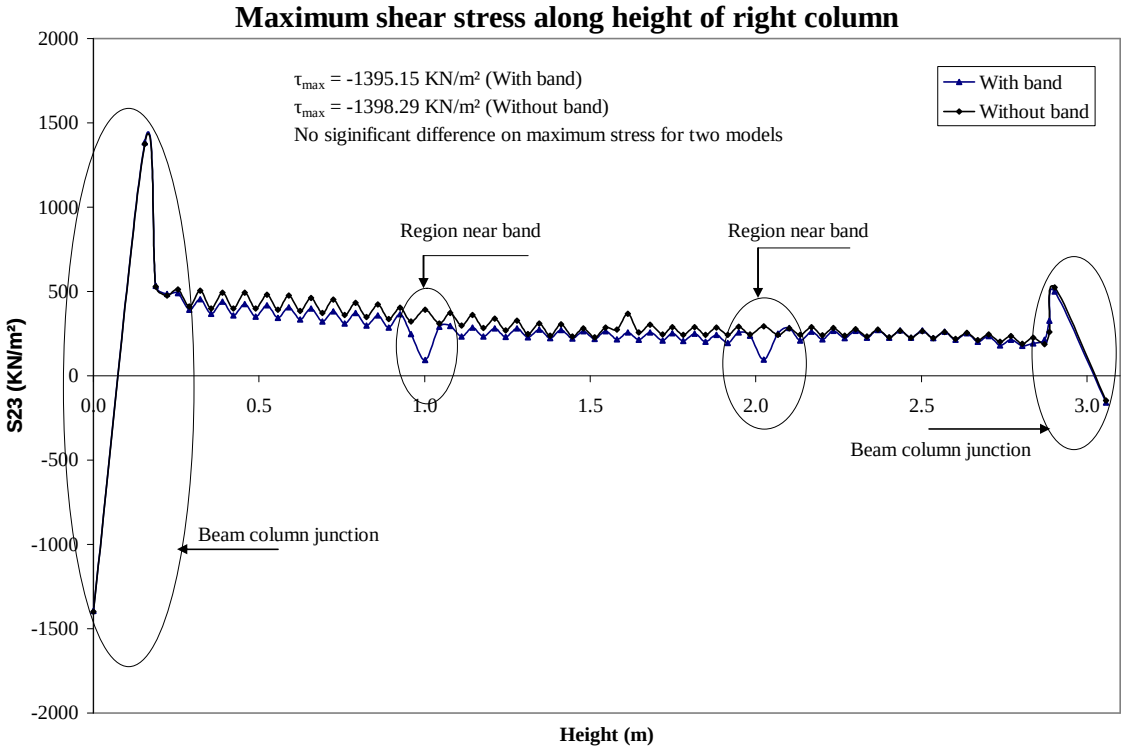

Fig-B29

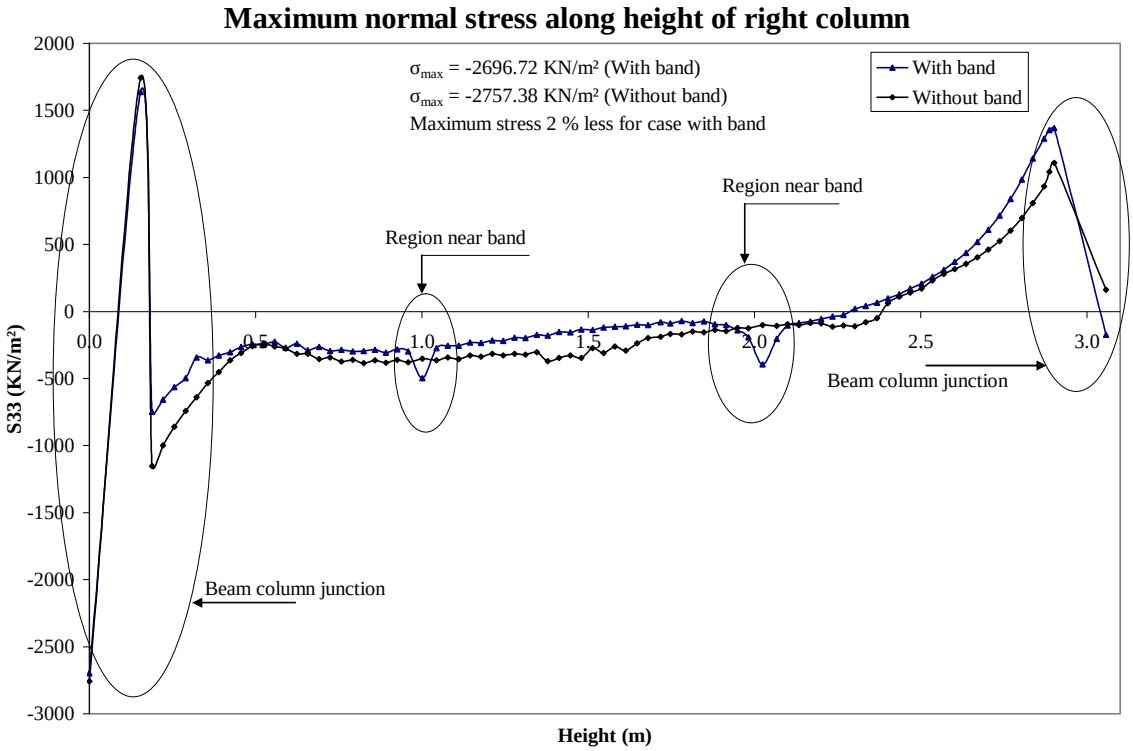

Fig-B30

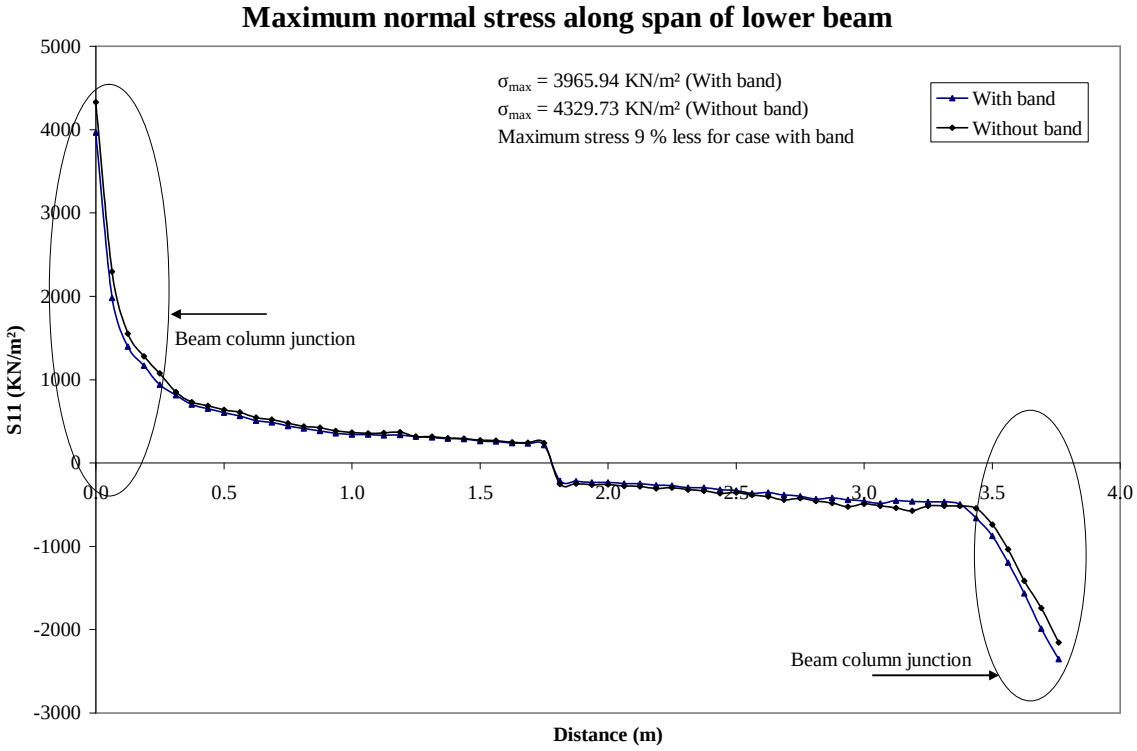

Fig-B31

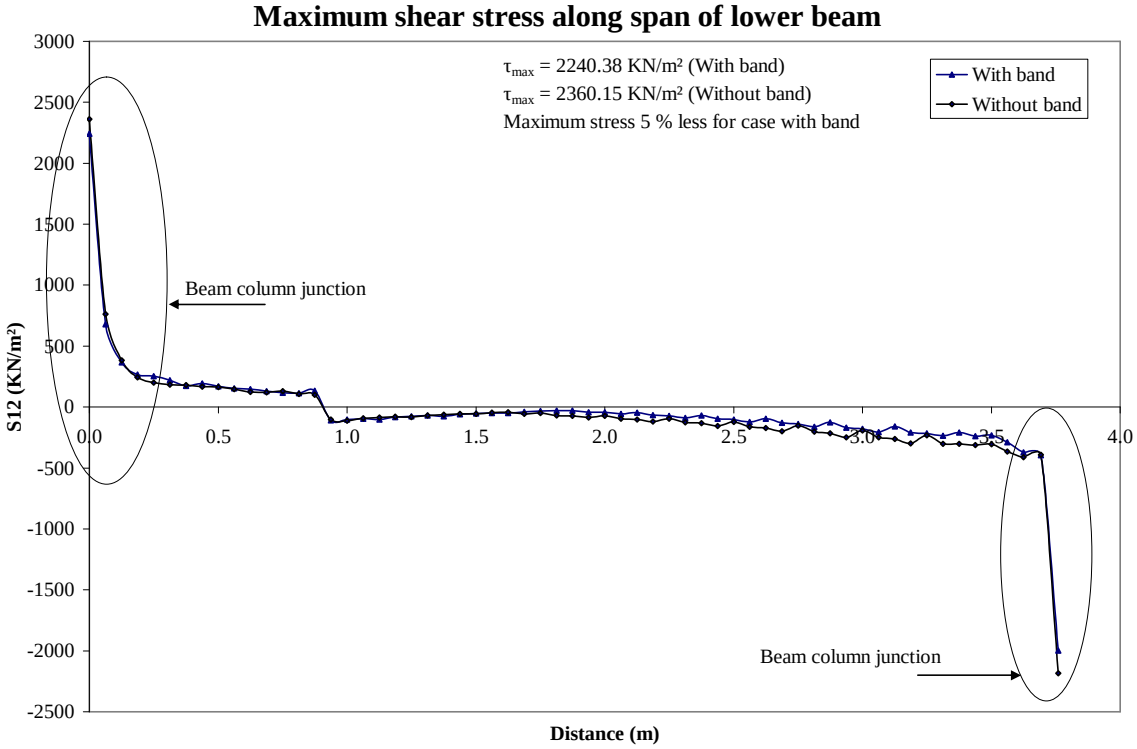

Fig-B32

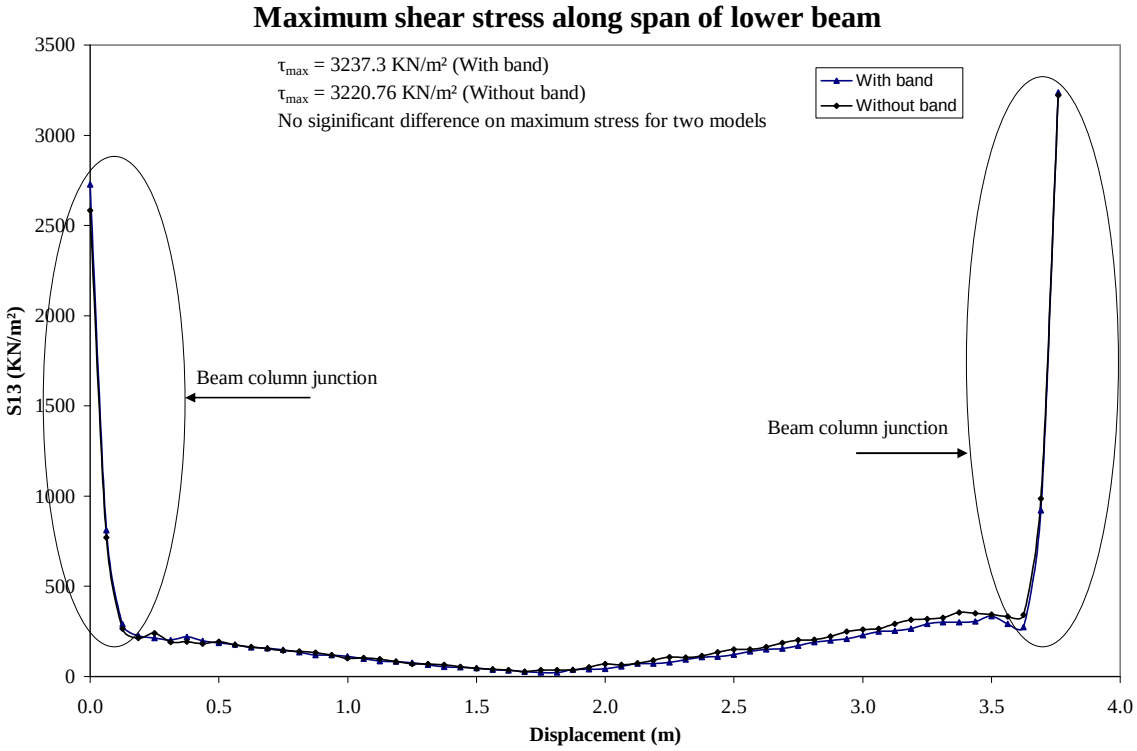

Fig-B33

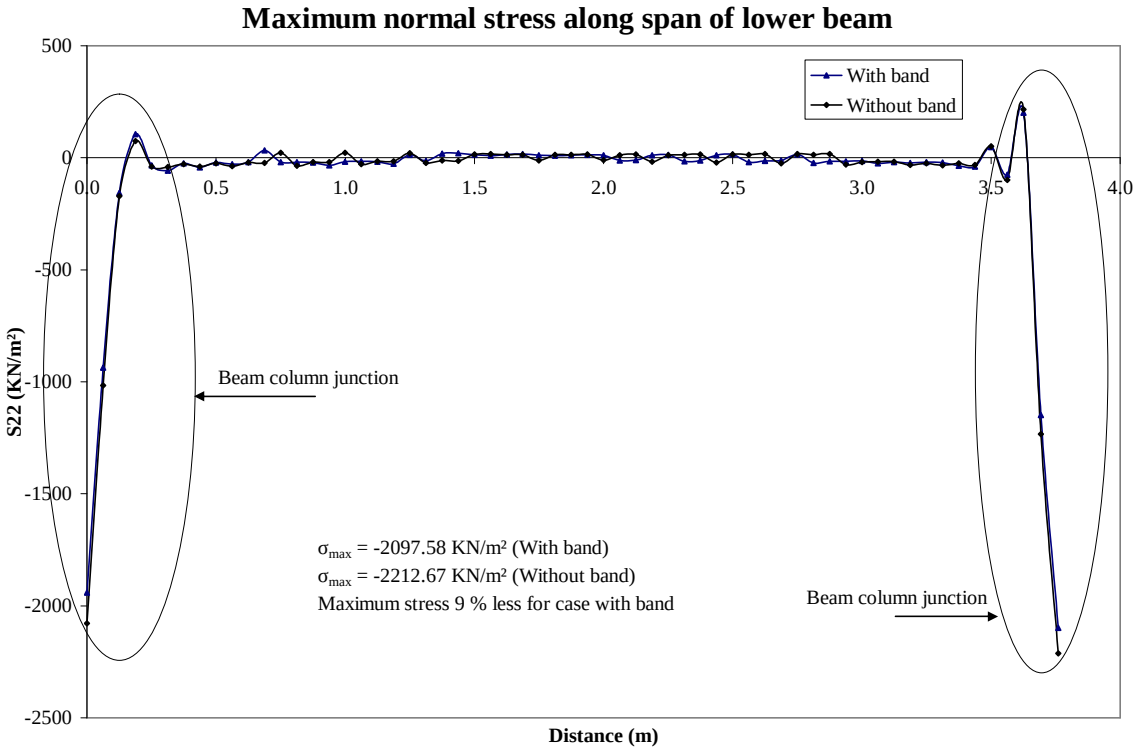

Fig-B34

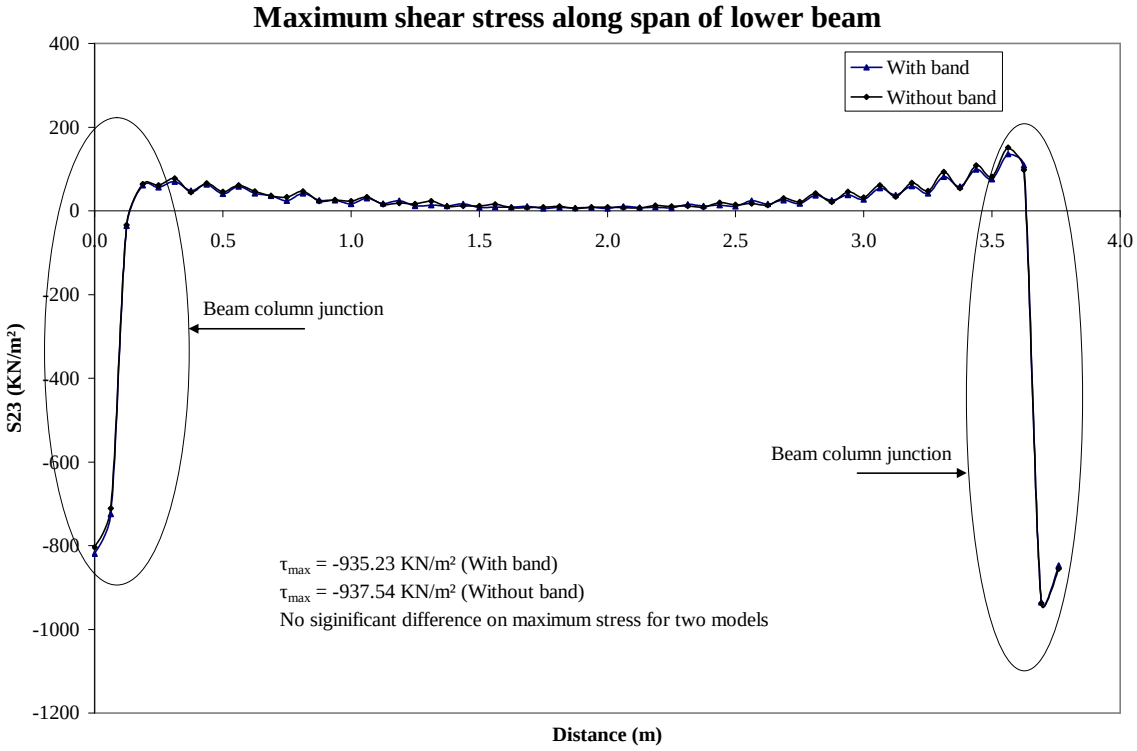

Fig-B35

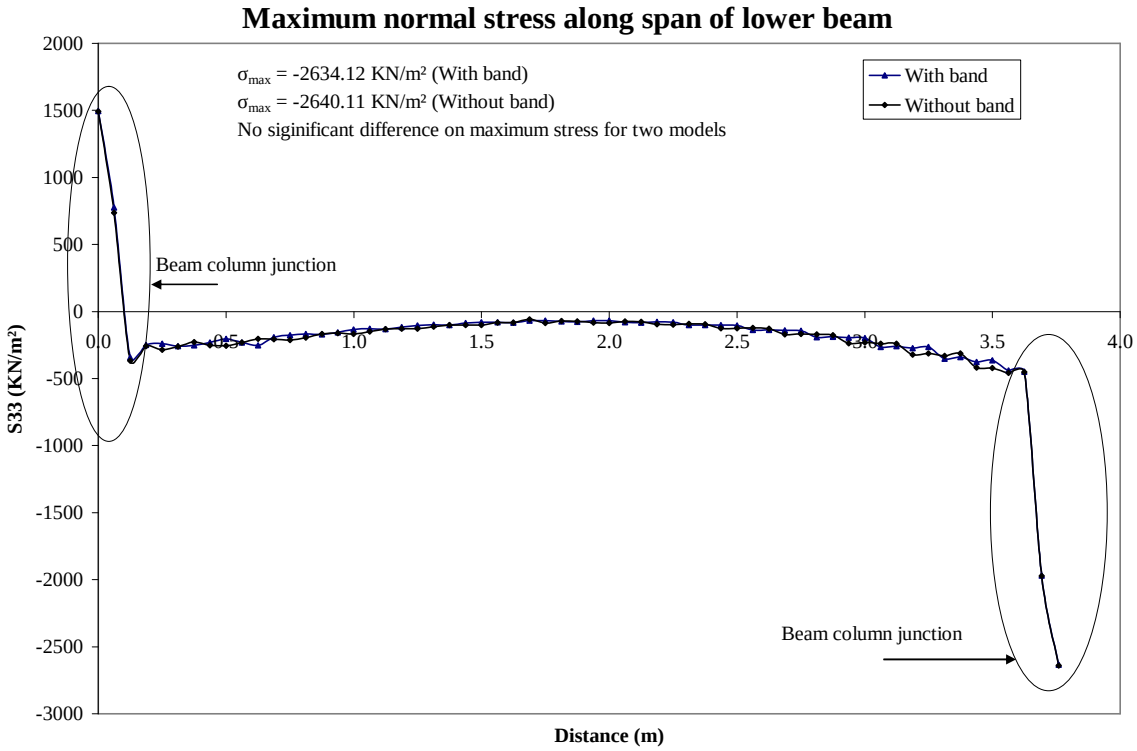

Fig-B36

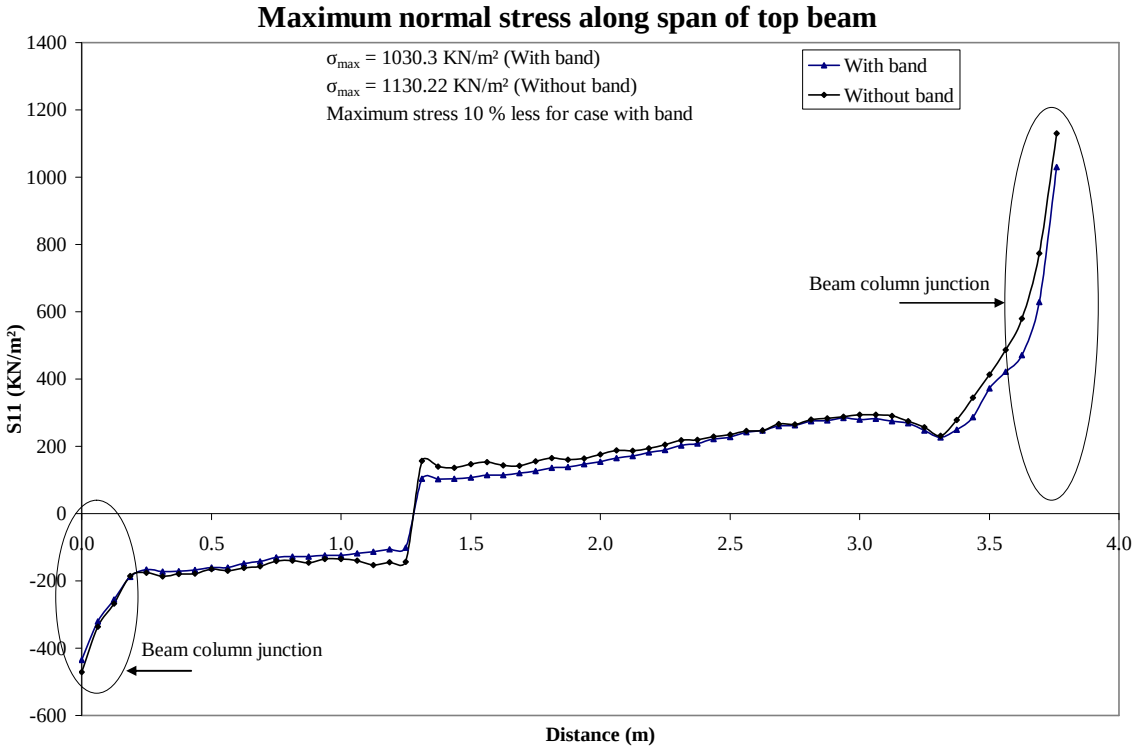

Fig-B37

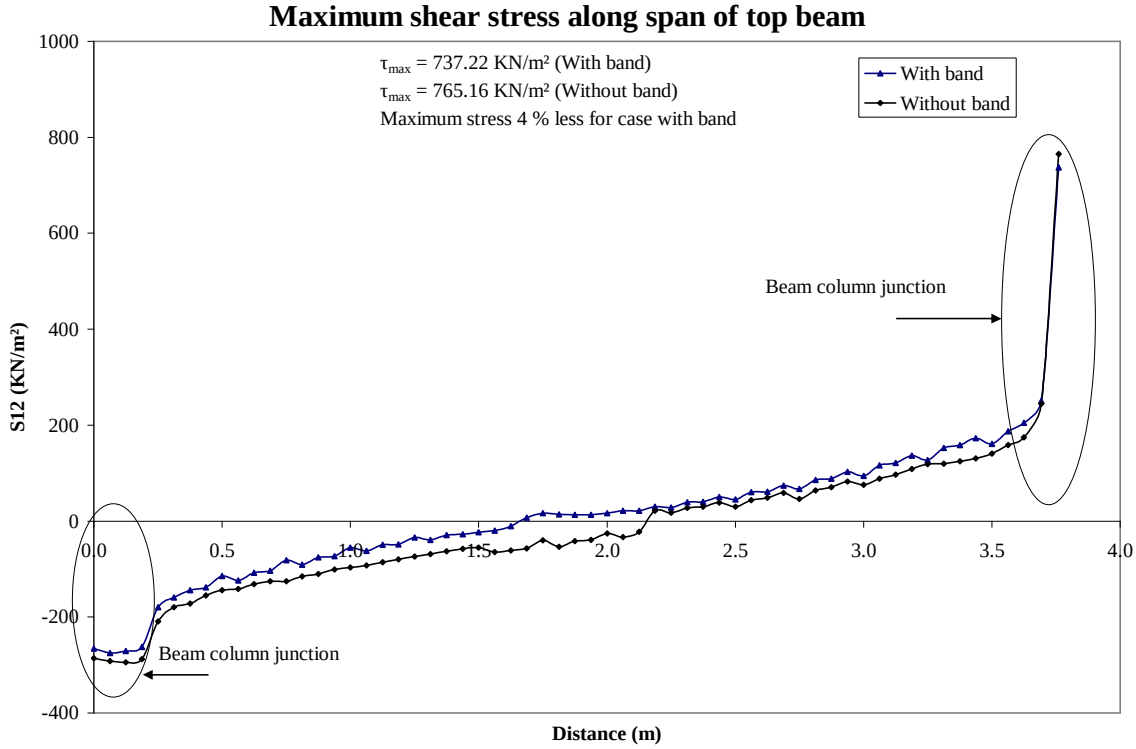

Fig-B38

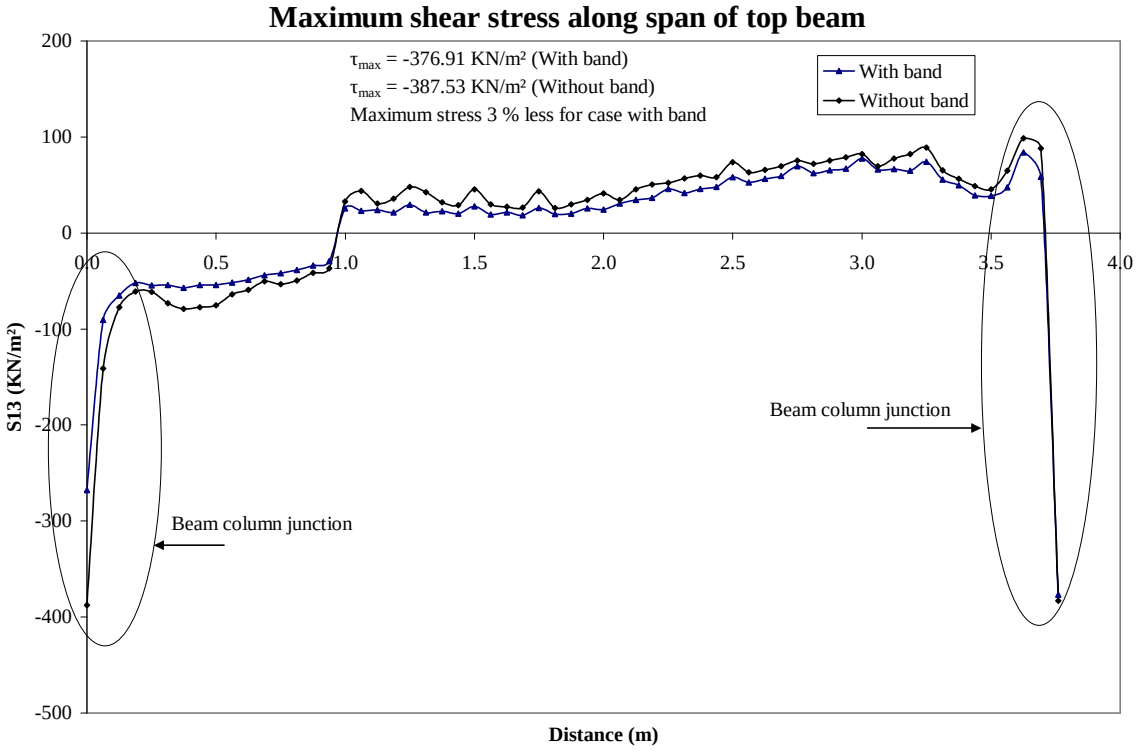

Fig-B39

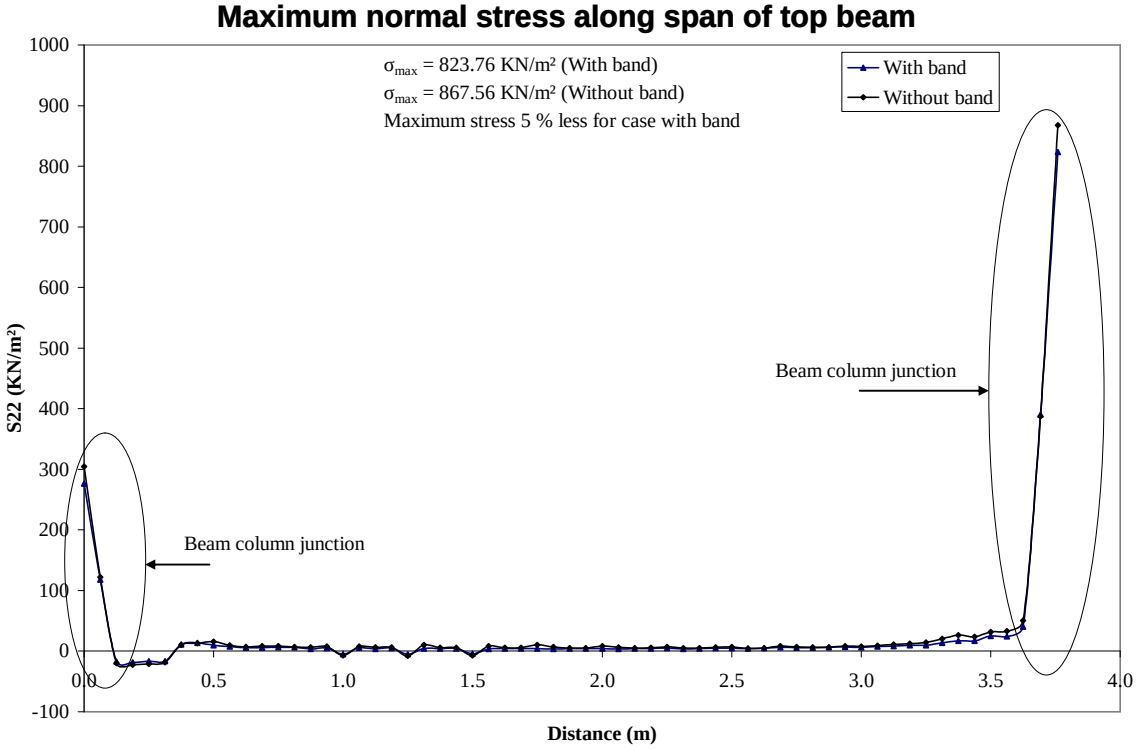

Fig-B40

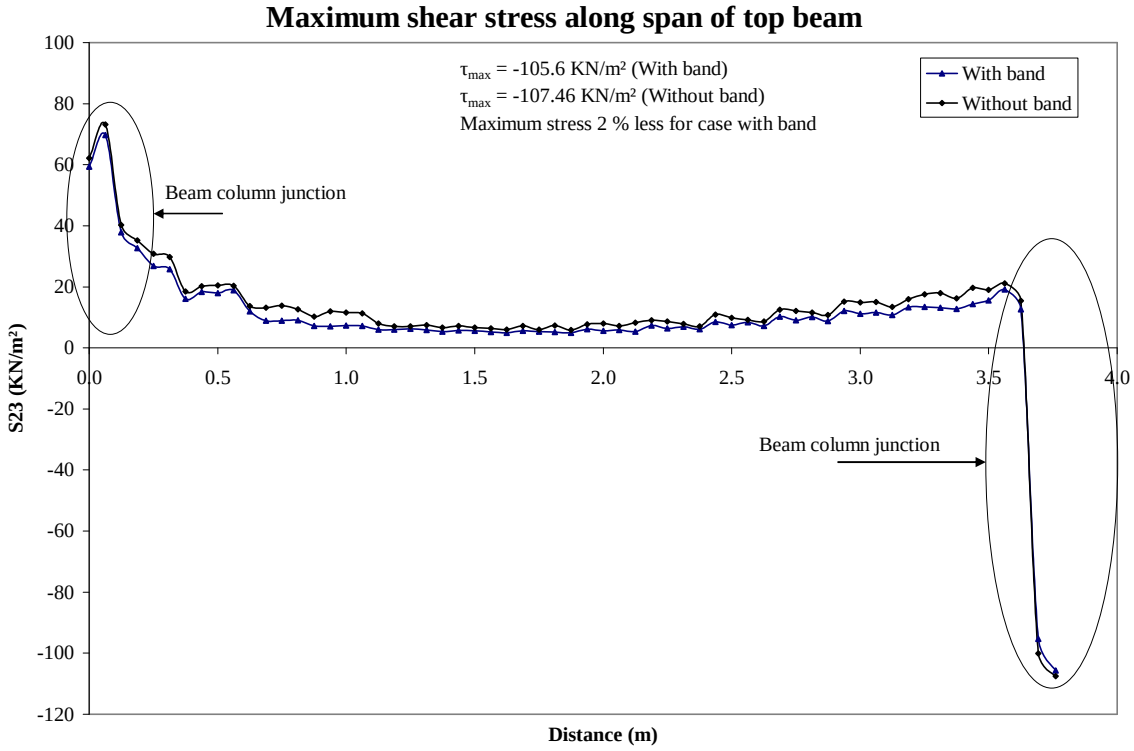

Fig-B41

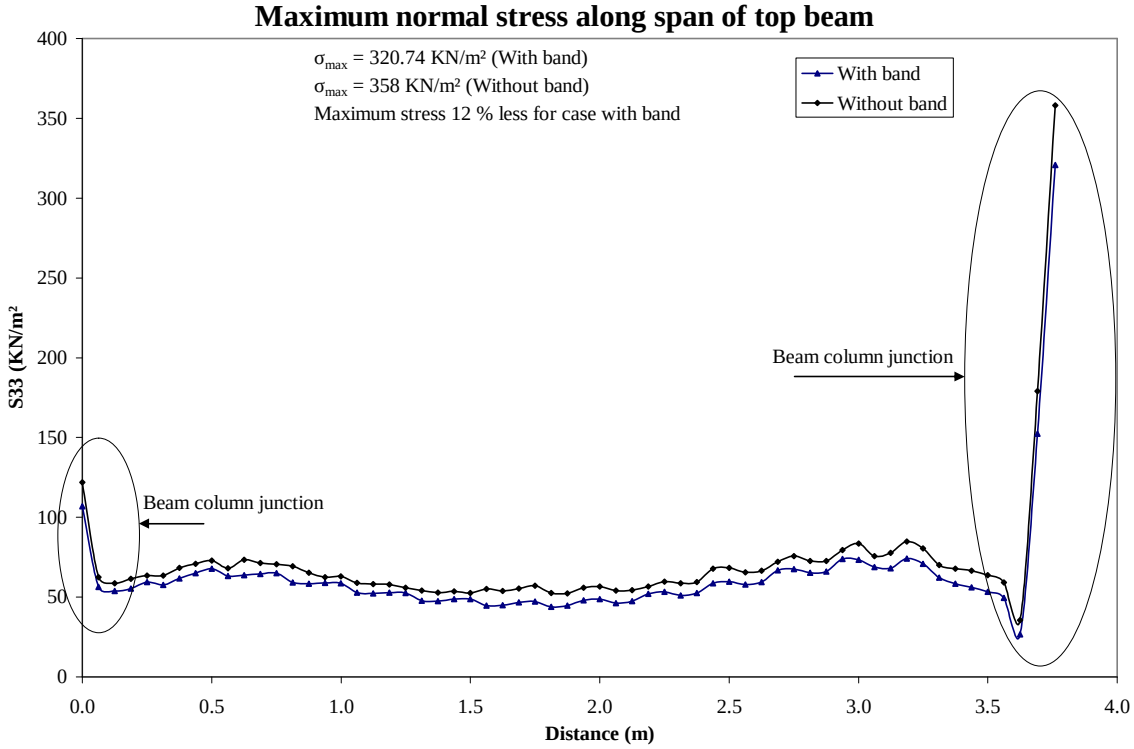

Fig-B42